

Article

Upstream-Downstream Influence of Water Harvesting Techniques (Jessour) on Soil Water Retention in Southeast Tunisia

Martin Calianno ^{1,2} , Tarek Ben Fraj ^{3,4}, Jean-Michel Fallot ¹, Mohamed Abbassi ^{3,5}, Aziza Ghram Messedi ^{3,5} , Hédi Ben Oueddou ^{3,5} and Emmanuel Reynard ^{1,*} 

¹ Institute of Geography and Sustainability and Interdisciplinary Centre for Mountain Research, University of Lausanne, Quartier Mouline, Géopolis, 1015 Lausanne, Switzerland

² Instituto Nacional de Tecnología Agropecuaria (INTA), Modesta Victoria 4450, San Carlos de Bariloche 8400, Argentina; calianno.martin@inta.gob.ar

³ CGMED Laboratory, University of Tunis, 94, BD du 9 avril 1938, Tunis 1007, Tunisia; abassi.med84@gmail.com (M.A.)

⁴ Faculty of Arts and Human Sciences, University of Sousse, Cité Erriadh, Sousse 4023, Tunisia

⁵ Faculty of Human and Social Sciences, University of Tunis, 4, BD du 9 avril 1938, Tunis 1007, Tunisia

* Correspondence: emmanuel.reynard@unil.ch

Abstract: Weather parameters and soil moisture profiles were measured at an hourly time step during four agricultural years (September to October, from 2018–19 to 2021–22) in two *Jessour* (water harvesting cultivated terraces) of the same valley in Zmertén (southeastern Tunisia), characterized by an arid climate. One instrumented *Jesr* (singular of *Jessour*) was located upstream and the other one downstream. During each dry season, when crops experience water stress, the downstream *Jesr* had a higher available water content than the upstream one; in the downstream *Jesr* the soil profile moisture remained above the wilting point, whereas in the upstream soil surface, moisture levels decreased to below the wilting point. High accumulation/low intensity rains (causing saturation/excess runoff) flooded both upstream and downstream *Jessour* from 50 mm of cumulative rainfall, whereas high intensity/low accumulation rains (causing infiltration/excess runoff) activated the downstream *Jesr* from an intensity of 15.2 mm/h, and a combination of moderate intensity and moderate accumulation rains activated both *Jessour* from an intensity of 8 mm/h and a cumulative rainfall of 33 mm. We propose to set 50 mm of cumulative rainfall and/or 6.4 mm/h of intensity as threshold values for the activation of the *Jessour* system in Zmertén. However, significant soil moisture recharges can occur even without activation of the *Jessour* system.

Keywords: water-harvesting technique; *Jessour*; soil moisture



Citation: Calianno, M.; Ben Fraj, T.; Fallot, J.-M.; Abbassi, M.; Ghram Messedi, A.; Ben Oueddou, H.; Reynard, E. Upstream-Downstream Influence of Water Harvesting Techniques (*Jessour*) on Soil Water Retention in Southeast Tunisia. *Water* **2023**, *15*, 1361. <https://doi.org/10.3390/w15071361>

Academic Editor: Adriana Bruggeman

Received: 13 February 2023

Revised: 23 March 2023

Accepted: 24 March 2023

Published: 1 April 2023



Copyright: © 2023 by the authors. Licensee MDPI, Basel, Switzerland. This article is an open access article distributed under the terms and conditions of the Creative Commons Attribution (CC BY) license (<https://creativecommons.org/licenses/by/4.0/>).

1. Introduction

Aridity and climate change are the major challenges faced by farmers who rely on rainfed farming [1]. On the Matmata-Dahar plateau in southeast Tunisia, the *Jessour* (plural of *Jesr*) are traditional water harvesting techniques that enable growing crops such as olive and almond trees in arid conditions [2,3]. In valleys with intermittent streams, successions of small dams are built to retain water runoff and sediments, forming terraces with sufficient soil depth to allow agriculture [4–6]. In the Dahar, most of the precipitation falls in short, high-intensity rainstorms [7] occurring in autumn. The role of the *Jessour* is to take advantage of these infrequent rainfalls to slow down runoff water thanks to the terraces system [8,9] and to increase soil moisture storage, prolonging the growing season for natural vegetation [4]. Only one effective rainfall annually can ensure adequate water supply for the rest of the hydrological year [10].

The present paper focuses on the soil moisture dynamics of *Jessour* and is the continuation of the work of Calianno et al. [11] that compared the ability of a *Jesr* to store soil

moisture in comparison with a similar site without a Jesr in the Dahar plateau (region of Zammour). On the one hand, previous works have already shown the quantified added value of water harvesting techniques on soil moisture using water balance or rainfall-infiltration modeling [12–15] and remote sensing [16]. Studies including on-site real-time soil moisture measurements exist for Jessour systems [4,10,17] and for various other techniques: micro catchments [18], stone barriers and earth bunds [19], and bench terraces [20]. A few studies combine on-site measurements with water balance modeling [21] or remote sensing [22]. The advantage of on-site measurements is that they constitute direct observations and so correctly portray soil moisture patterns at the scale of the water harvesting technique, but the drawback is that the data is taken manually and is therefore of poor temporal resolution (at best, weekly). On the other hand, modeling and remote sensing techniques give soil moisture estimates on a broader spatial scale and allow a finer temporal resolution, but they are not suitable to describe small-scale processes within the Jessour system (dams and terraces, soil profiles, infiltration, runoff). Finally, socio-hydrology works on water harvesting usually consider the influence of multiple structures (water harvesting pounds, irrigation systems) in upstream–downstream watershed dynamics, studying the impact of groups of users upstream on water availability for downstream users [23]. Such studies are usually at the watershed scale, from the perspective of ecosystem services and use a modeling approach [24], while practical field analyses are rare or limited to the social aspects (participatory approach, questionnaires, interviews) [25]. Information on hydrological parameters is lacking to allow the impact assessment of water harvesting techniques on soils.

The present study investigates the upstream–downstream influence in a micro-scale watershed (a Jessour system of less than 1 km²), focusing on the impact of a series of terraces on soil moisture. Water content sensors combined with data loggers are used to provide on-site measurements at the scale of the agricultural plot that are continuous over a long period (4 years) and at hourly time steps, without disturbing the soil properties.

The first objective of this research is to compare the soil moisture retention of a Jesr situated upstream of a valley and a Jesr downstream. The second objective is to identify the characteristics of the effective rainfall events able to activate the Jessour system (i.e., trigger runoff through the succession of terraces). Two measurement stations were installed in the same valley (one in an upstream Jesr, the other downstream, in the last Jesr) from September 2018 to September 2022. The measurements included a 1.25 m deep soil moisture profile and weather data as well as soil samples providing soil texture and organic matter content.

Study Area

The Jessour instrumented in this study are located in the village of Zmertén, in southeast Tunisia. Zmertén is part of the Toujane municipality, located on the Matmata-Dahar plateau (Figure 1). This “Djebel” (Tunisian for “mountain”), is situated between the Jeffara plain, bordering the Mediterranean Sea, and the eastern limits of the Sahara. It culminates at 713 m a.s.l. and is composed of a system of cuestas that gently incline to the west and are partly dissected by valleys and depressions filled with several-meter thick Quaternary fine sand and silt (or loess) [26–29]. Zmertén lies at an altitude of 530 m a.s.l. and is located in the valley of Wadi Zmertén that dissects the dolomitic cuesta back slope. Due to steep valley slopes, fine sand and silt deposits in Zmertén are thinner than in other areas of the Matmata-Dahar plateau. In the tributaries of Wadi Zmertén, they are less than one meter thick. At the valley floors of the main Wadi, they are up to 4 m thick [28,29]. These fine deposits are the agricultural “wealth” of the Dahar that otherwise would lack soils deep enough for annual crops [2,30].

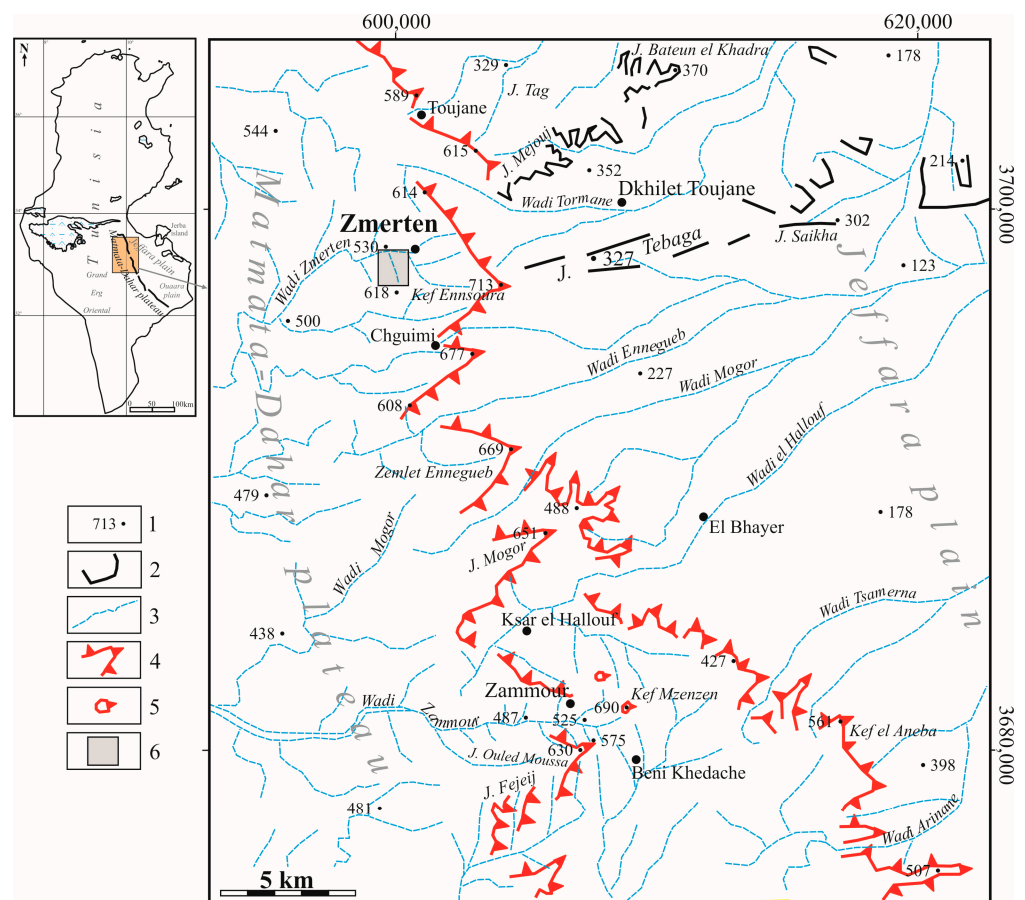


Figure 1. Location and general geomorphological context of the study area (Zmertem) on the Matmata-Dahar plateau (southeast Tunisia). 1. Altitude, 2. Talus, 3. Wadi (intermittent stream), 4. Cuesta, 5. Witness butte, 6. Studied site.

The Matmata-Dahar plateau lies in the upper arid bioclimatic region [31] and is located in the transition zone between the Sahara to the southwest with a subtropical, dry and hot climate, and central Tunisia to the north, which is influenced by a relatively temperate Mediterranean climate [5]. The rainfall regime is of Mediterranean type with the rainy season extending from September to April. There are few rainy days (on average 30 to 40 days per year) but rainfall events can be of high intensity, with 20-year-return period maximum rainfalls exceeding 100 mm/day [7]. Summers are hot, with average temperature in July–August between 29 and 30 °C. Due to the Sahara’s dry and hot winds, temperatures can reach up to 40 to 50 °C and reduce air humidity down to 10% [32]. This dry climate, combined with hot temperatures, causes significant evapotranspiration rates, with values above 2000 mm/year in Beni Khedache (20 km south of Zmertem; see Figure 1) [33]. Such severe climatic conditions impose a deficit climatic water balance [5] that is very constraining for rain-fed agriculture and led to the development of water-harvesting techniques such as the Jessour [2,12,34].

2. Materials and Methods

2.1. Description of the Jessour System

The Jessour form a hydraulic unit made of three main components: (i) a dam (locally called *Tabia* or *Ketra*) between 2 and 5 m high and between 15 and 50 m long across the talweg [2], in the form of a small earth embankment, sometimes reinforced with stones, with a lateral spillway (called a *Menfes*) or a central spillway (called a *Masraf*) made of stones; (ii) a terrace which includes the cropping area (called *Khliiss*); and (iii) an impluvium, which is the runoff sub-catchment area [2,11,35,36]. The Jessour take advantage of short

rainfall events occurring in autumn and winter by collecting and slowing down runoff generated at the level of the impluviums [11]. In the wet season, when the soil is well supplied with water, the upper horizons provide water to fruit trees (olives, almonds, figs) and potential intercropping (lentils, peas, oats). However, during the summer period, the deep horizons provide water to fruit trees to better withstand dry episodes [10]. Besides agriculture they play a role in aquifer recharge, via runoff water infiltration into the terraces and flood control, and protect infrastructure and towns built downstream [37]. The Jessour are usually situated one after another along a valley talweg and form terraces overflowing into one another after intense rainfall events. This system favors deep infiltration and enhances soil water storage by forming temporary ponds and creating a small aquifer in each Jesr [11]. The accumulation of sediments (silts and fine sand) behind the dams also provides nutrients to crops [12].

2.2. Instrumented Sites

To highlight the effect of water collection by the Jessour according to the impluvium area, two measurement stations were placed in the same valley: in a Jesr located upstream and in a Jesr located downstream (Figure 2).

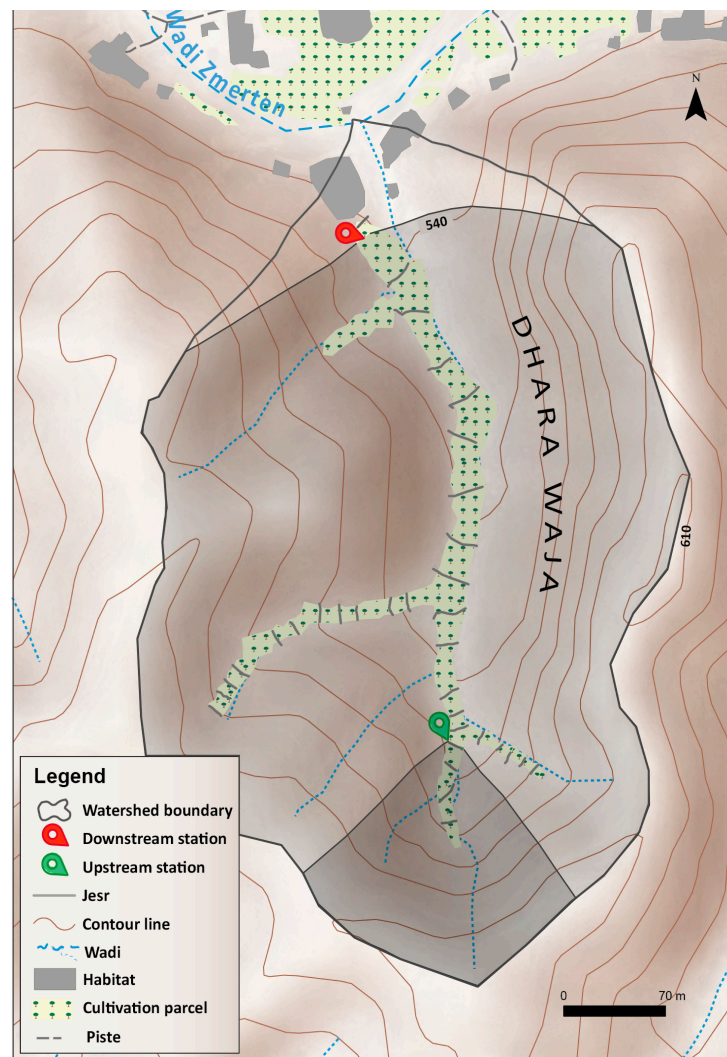


Figure 2. Location of the two measurement stations in Jessour situated in the upstream and downstream sections of Dhara Waja ravine (*Chaabet* in Arabic), with their respective impluvium.

The two stations were installed in the same ravine: the Chaabet Dhara Waja sub-catchment, a tributary of the Wadi Zmertem. Dhara Waja is a narrow, 70 m deep ravine with homogeneous characteristics concerning local geology, soil texture, climate and impluvium topography (Figure 3a). The ravine dissects Turonian and Cenomanian dolomite, limestone, clay and gypsum series. It originates at an altitude of 618 m a.s.l. and its confluence with Wadi Zmertem is at an altitude of 530 m. The longitudinal profile of the talweg shows an average slope of 13%, with a value of 30% for the first 200 m upstream. Much steeper slopes of around 56% characterize the transverse profile. Due to the steep slopes of the valley, Quaternary deposits are limited. They take the form of localized colluvium taking on the appearance of a lithosol-rendzinas type soil [38]. At the bottom of the ravine, Quaternary heritage appears in the form of superimposed levels of brecciated conglomerate, fine sand and silt sealed by a calcareous crust and friable colluvium. The deposits accumulated in the Jessour terraces mainly have a loam texture.



Figure 3. General view of the Dhara Waja ravine (a). View of downstream (b), and upstream Jessour (c). Photos: E. Reynard and T. Ben Fraj.

There are 23 Jessour in the main ravine of Dhara Waja. In the tributaries of Dhara Waja there are 24 structures (smaller Jessour, dry stone weirs and walls that reduce the force of runoff during heavy rains and protect the Jessour and other infrastructure located downstream). Fine sand and silt being rare in Zmertem, the Tabias (dams) of these Jessour are made of dry stones. The downstream station is placed in the last (23rd) Jesr of the ravine (see Figure 2). The upstream measuring station is placed in the sixth Jesr counted from upstream for the reason that the cultivable surface and the depth of the deposits of the upper Jessour are too small to allow easy installation of the sensors.

The upstream Jesr has an impluvium of 16.000 m² and a terrace of 100 m², and the downstream Jesr has an impluvium of 158.000 m² and a terrace of 570 m². Due to its small size, the upstream terrace only hosts a small fig tree and a small olive tree (Figure 3c), whereas downstream, the terrace hosts 7 large fig and olive trees (Figure 3b).

2.3. Experimental Setup

The field campaign lasted four years, with continuous measurements from 24 September 2018 to 11 September 2022. Each measurement site consists of a weather station and a 1.25 m deep soil pit equipped with soil moisture sensors (Figure 4).

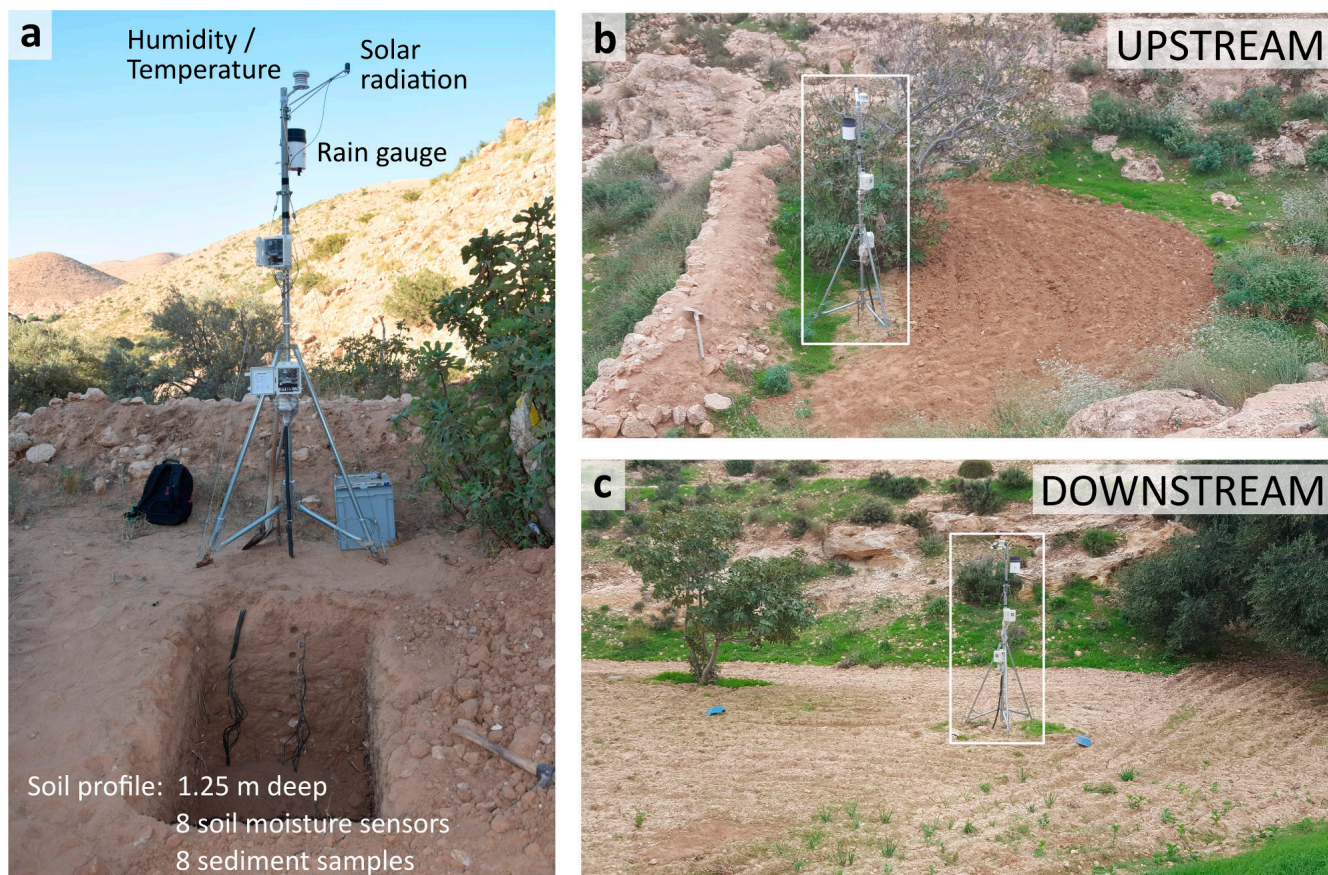


Figure 4. Configuration of the measurement station (a); location in upstream Jesr (b) and downstream Jesr (c). Photos: T. Ben Fraj and M. Abbassi.

Due to the small size of the upstream terrace, the measurement station was installed next to the dam and close to the Jesr's fig tree (at about 1 m distance, see Figure 4b). We wanted to occupy as little space as possible on the cropping area so as not to disturb the farming activity. The downstream station is located in the center of the cropping area, approximately 5 m from the closest olive tree (Figure 4c).

The meteorological stations consisted of a bucket rain gauge, a sheltered sensor measuring humidity and temperature and a pyranometer measuring solar radiation (Figure 4a, Table 1). A data logger recorded the meteorological parameters at an hourly time step. The soil stations were equipped with height volumetric water content sensors, placed every 15 cm in the soil pit to create a soil moisture profile. After installation, the soil pit was refilled with the original sediments. The first sensor was placed 20 cm below the soil surface. The soil moisture sensors used were the ECH2O probe model EC-5 (Decagon Devices Inc., Pullman, WA) and used the capacitance method to make an indirect evaluation of the volumetric water content [39]. Their volume of influence is 0.3 L (each sensor measures in a sphere of 0.3 L). This means that the soil moisture is estimated until 4.15 cm above and

below each sensor. A data logger recorded soil moisture parameters at a two-hour time steps. The advantage of this setup over manual measurements is the continuity and high frequency of the measurements. In addition, as the trench is filled, it gives soil moisture values with minimal modification of the Jessour hydrological functions (runoff, infiltration), and there is no bias due to the drying of the soil section.

Table 1. Devices installed on the measurement stations, measured parameters, units and chosen time steps.

Device	Measured Parameter	Unit	Time Step
Meteorological station			
Pyranometer	Solar radiation	W/m ²	1 measurement/1 h
Bucket rain gauge	Rainfall	mm	1 measurement/1 h
Sheltered sensor	Temperature	°C	1 measurement/1 h
Sheltered sensor	Relative humidity	%	1 measurement/1 h
Soil station (8 sensors and 8 samples, every 15 cm)			
ECH ₂ O sensors: measurement based on the capacitance technique	Volumetric water content (θ)	m ³ /m ³ (water vol./soil vol.)	1 measurement/2 h
Soil samples (laser granulometry)	Soil texture	% Clay, % Silt, % Sand	
Soil samples (Rock-Eval pyrolysis)	Total organic carbon	% Organic Matter (% OM)	

In parallel, soil samples were collected next to each water content sensor for laboratory analysis, where soil textures were obtained through laser granulometry. The range of particle sizes for soil texture is based on the WRB classification, i.e., clay (<0.002 mm), silt (0.002–0.063 mm) and sand (0.063–2 mm) [34]. Finally, the proportion of organic matter (% OM) in soil samples was provided by the Rock-Eval pyrolysis technique [40].

2.4. Calculation of Soil Water Content Values

The available water content (*AWC*) is the amount of water contained in the soil that can be reached and extracted by plants. It is a useful parameter to evaluate the ability of the Jessour to harvest and store soil water. The *AWC* comprises the values of soil moisture between the wilting point (θ_{WP}) and soil moisture at field capacity (θ_{FC}) [41].

$$\theta_{WP} < AWC < \theta_{FC} \quad (1)$$

Above field capacity, the soil is saturated in water and the plant can be asphyxiated. Below wilting point, the plant does not have sufficient root suction forces to absorb water [11].

The soil moisture at field capacity is the amount of soil moisture or water content held in the soil after excess water has drained away and the rate of downward movement has decreased. This usually takes place 2 to 3 days after rain or irrigation in pervious soils of uniform structure and texture: the water is retained in the soil by suction [42]. For the majority of plants grown under a temperate climate, the field capacity is defined as the bulk water content retained in soil at −0.33 bar of suction pressure [43].

The soil moisture at wilting point is the minimal level of soil moisture the plant requires not to wilt. At moisture levels below this, the plant has insufficient suction forces to withdraw water from the soil. The physical definition of the wilting point is the water content at −15 bar of suction pressure [43].

In the Jessour, θ_{WP} and θ_{FC} are estimated for each soil layer (i) using Rawls' formulas [41]. These empirical relations are based on soil texture (% Sand; % Clay) and organic matter content (% OM).

$$\theta_{FC}(i) \left[m^3/m^3 \right] = \frac{257.6 - (2 * \%_{Sand}(i)) + (3.6 * \%_{Clay}(i)) + (29.9 * \%_{OM}(i))}{1000} \quad (2)$$

$$\theta_{WP}(i) \left[m^3/m^3 \right] = \frac{26 + (5 * \%_{Clay}(i)) + (15.8 * \%_{OM}(i))}{1000} \quad (3)$$

From volumetric soil moisture data, the AWC is calculated for each soil layer (i) as follows: When $\theta(i) \geq \theta_{FC}(i)$:

$$AWC(i) \left[m^3/m^3 \right] = \theta_{FC}(i) - \theta_{WP}(i) \quad (4)$$

When $\theta_{WP}(i) < \theta(i) < \theta_{FC}(i)$:

$$AWC(i) \left[m^3/m^3 \right] = \theta(i) - \theta_{WP}(i) \quad (5)$$

When $\theta(i) \leq \theta_{WP}(i)$:

$$AWC(i) \left[m^3/m^3 \right] = 0 \quad (6)$$

Then values are summed for the whole 1.25 m deep soil profile:

$$AWC[mm] = \sum_{i=1}^n h(i)AWC(i) \quad (7)$$

If soil moisture data are not available (for instance due to sensor malfunction) the AWC is estimated using the value of the nearest functioning sensor.

2.5. Recharge, Drying and Activation of the Jessour

We define the Jessour recharge as the AWC gained in the soil column (1.25 m) after a rainfall event and the drying as the AWC lost during dry periods. The Jessour activation occurs when the rain provokes runoff and the accumulation of water in the terraces of a Jessour system. Runoff water flows from one terrace to another according to the height of Jessour spillways, which are dimensioned by locals to ensure the reasonable sharing of water. We estimate that there is activation when the shallowest soil moisture sensor (S1) reaches the saturation value ($0.40 m^3/m^3$). There can be two ways to reach the Jessour activation: saturation/excess runoff when rainfall intensity is low but the accumulation is sufficient to saturate the soil column (especially if the soil is already moist), or infiltration/excess runoff when rainfall intensity exceeds the infiltration capacity of the soil surface.

2.6. Calculation of Potential Evapotranspiration

The formula of Turc [44] was used to calculate a daily potential evapotranspiration (ET_0) time series from solar radiation (Rad) ($cal/cm^2/day$), relative humidity (RH) (%) and mean daily temperatures data (T) ($^{\circ}C$):

When $RH \geq 50\%$:

$$ET_0[mm] = 0.013(Rad + 50) \left(\frac{T}{T + 15} \right) \quad (8)$$

When $RH < 50\%$:

$$ET_0[mm] = 0.013(Rad + 50) \left(\frac{T}{T + 15} \right) \left(1 + \frac{50 - RH}{70} \right) \quad (9)$$

The Turc formula was chosen because it is a robust empirical method that requires less data than the Penman formula. Moreover, it is suitable for arid regions. In their comparative study of evapotranspiration formulas applied to southern Tunisia climatic data, Damagnez et al. found that the Turc formula gave results similar to the Penman formula [45].

3. Results

3.1. Characteristics of Soil Layers

In the upstream Jesr, the sedimentary sequences contain coarse elements from the size of gravel to small blocks of 10 cm of diameter of limestone and dolomite. The soil profile is dominated by a silt loam structure that was observed next to the four shallowest sensors (from -20 cm to -65 cm) and the deepest sensor (at -125 cm). Two samples show a sandy loam texture (from -95 cm to -100 cm) and one shows a loam texture (at -80 cm) (Table 2). The organic matter content varies between 0.38 and 0.68%, with higher values near the soil surface (S1, S2 and S3 above 0.54 %).

Table 2. Soil sample analysis for each layer in upstream and downstream profiles: texture class, organic matter content and soil moisture content at field capacity (θ_{FC}) and at wilting point (θ_{WP}).

Sensors	Soil Layer Thickness	Texture (WRB Class)	Clay (%) <0.002 mm	Silt (%) 0.002–0.063 mm	Sand (%) 0.063–2 mm	Organic Matter (%)	θ_{FC} (m ³ /m ³)	θ_{WP} (m ³ /m ³)
Upstream								
S1 (-20 cm)	20 cm	Silt Loam	10.3	67.3	22.4	0.67	0.27	0.09
S2 (-35 cm)	15 cm	Silt Loam	10.5	65.6	23.8	0.54	0.26	0.09
S3 (-50 cm)	15 cm	Silt Loam	9.5	68.2	22.3	0.68	0.27	0.08
S4 (-65 cm)	15 cm	Silt Loam	12.2	63.8	24.0	0.38	0.26	0.09
S5 (-80 cm)	15 cm	Loam	9.3	49.5	41.2	0.42	0.22	0.08
S6 (-95 cm)	15 cm	Sandy Loam	6.1	39.2	54.7	0.49	0.18	0.06
S7 (-110 cm)	15 cm	Sandy Loam	6.0	32.4	61.5	0.44	0.17	0.06
S8 (-125 cm)	15 cm	Silt Loam	11.9	58.5	29.6	0.50	0.26	0.09
Downstream								
S1 (-20 cm)	20 cm	Silt Loam	13.3	79.1	7.7	1.36	0.33	0.11
S2 (-35 cm)	15 cm	Silt Loam	11.3	65.5	23.2	0.82	0.28	0.10
S3 (-50 cm)	15 cm	Silt Loam	11.7	59.9	28.5	0.58	0.26	0.09
S4 (-65 cm)	15 cm	Silt Loam	8.4	55.6	36.0	0.66	0.24	0.08
S5 (-80 cm)	15 cm	Sandy Loam	3.9	25.4	70.7	0.32	0.14	0.05
S6 (-95 cm)	15 cm	Silt Loam	12.3	71.4	16.3	0.59	0.29	0.10
S7 (-110 cm)	15 cm	Sandy Loam	6.5	34.7	58.8	0.25	0.17	0.06
S8 (-125 cm)	15 cm	Loam	7.8	42.2	50.1	0.10	0.19	0.07

In the downstream Jesr, the coarse load is no bigger than gravels of 3 cm in diameter and contains mostly millimetric to centimetric limestone granules. The four shallowest layers (-20 cm to -65 cm) are affected by 2 cm wide cracks and have the highest clay and silt content. These cracks correspond to desiccation cracks that opened during the dry season given that the trench was dug in September 2018. The texture is similar to that of the upstream Jesr, with five samples of silt loam, two samples of sandy loam and one single sample of loam (Table 2). As in the upstream Jesr, the organic matter content is higher near the surface. Values range from 0.10 to 0.25% in the deepest layers (-110 cm to -125 cm), from 0.32 to 0.66% next to sensors 3 to 6 (-50 cm to -95 cm). 0.82% was measured at -35 cm and 1.36% close to the surface (-20 cm).

As the particle size analysis is limited to grain sizes smaller than sands, it is important to note the richness in coarse elements in the upstream Jesr profile since it is located closer to the rock debris supply zone and on a steeper slope than the downstream Jesr.

3.2. Hydro-Meteorological Characteristics of the Four Observed Agricultural Years

Rainfall, temperature, evapotranspiration (ET₀), soil profile recharge and drying are first analyzed annually, for the upstream and downstream Jessour (Table 3). The difference between recharge and drying gives the annual trend.

Table 3. Annual meteorological values for the upstream/downstream Jessour for the four observed agricultural years (September–October): rainfall, temperature, evapotranspiration, recharge and drying of the 1.25 m soil profile. Mean annual rainfall and temperature in Beni Khedache (1990–2004) in southeast Tunisia, according to the National Meteorological Institute of Tunisia [33].

Agricultural Year (Sept-Aug)	2018–19 Up/Down	2019–20 Up/Down	2020–21 Up/Down	2021–22 Up/Down	Beni Khedache (1990–2004)
Rainfall (mm)	176/195	303/318	235/260	n.a./124	271
Temperature (°C)	18.1/17.8	19.2/18.9	19.8/19.6	19.4/19.1	20.1
ET ₀ (mm)	1332/1320	1458/1454	1473/1464	1457/1453	
Recharge (mm)	329/324	386/331	365/448	23/10	
Drying (mm)	303/283	375/319	371/476	9/5	
Difference Recharge-Drying (mm)	26/41	10/12	−6/−27	14/5	

Considering the upstream/downstream differences, these values show slightly more evapotranspiration and slightly higher temperatures upstream. Concerning rainfall, there is 5% to 10% difference between the upstream and downstream pluviometers: rainfall values are a little higher downstream. During the last year of measurement (2021–2022), the upstream pluviometer showed technical problems and started to give erroneous data, so for that period, the downstream rainfall data were used for both sites.

In relation to seasonal differences, with cumulative rainfall of 176/195 mm (upstream/downstream values) and evapotranspiration of 1332/1320 mm, 2018–19 was relatively dry; it was also the coolest of the four observed agricultural years (18.1/17.8 °C). The soil profile recharge (329/324 mm) was lower than during the two following years, but this was compensated with lower drying (303/283 mm). These conditions resulted in the highest balance between recharge and drying (+26/+41 mm).

2019–20 was humid and hot (considering the arid climate) with cumulative rainfall of 303/318 mm, an average temperature of 19.2/18.9 °C and 1458/1454 mm of evapotranspiration. That year, the soil profile recharge (386/331 mm) was similar to its drying (375/319 mm).

2020–21 was the hottest year (19.8/19.6 °C). High values of evapotranspiration (1473/1464 mm) provoked the most intense drying (371/476 mm). The highest recharge values were also observed (365/448 mm), although it was not the rainiest year (235/260 mm).

2021–22 was the driest agricultural year (n.a./124 mm) and the recharge was extremely low (only 23/10 mm), indicating that there was almost no effective rainfall that year. These observations show that rainfall data need to be analyzed at a finer temporal scale to evaluate the recharge of Jessour terraces.

3.3. Soil Moisture Dynamics in Upstream and Downstream Jessour

The evolution of soil moisture for the eight sensors in the upstream and downstream soil profiles is analyzed here for each agricultural year in relation to rainfall events (Figures 5–8). Typical threshold values are also shown in the figures: soil moisture at wilting point (θ_{WP}), at field capacity (θ_{FC}), and at saturation (θ_{SAT}).

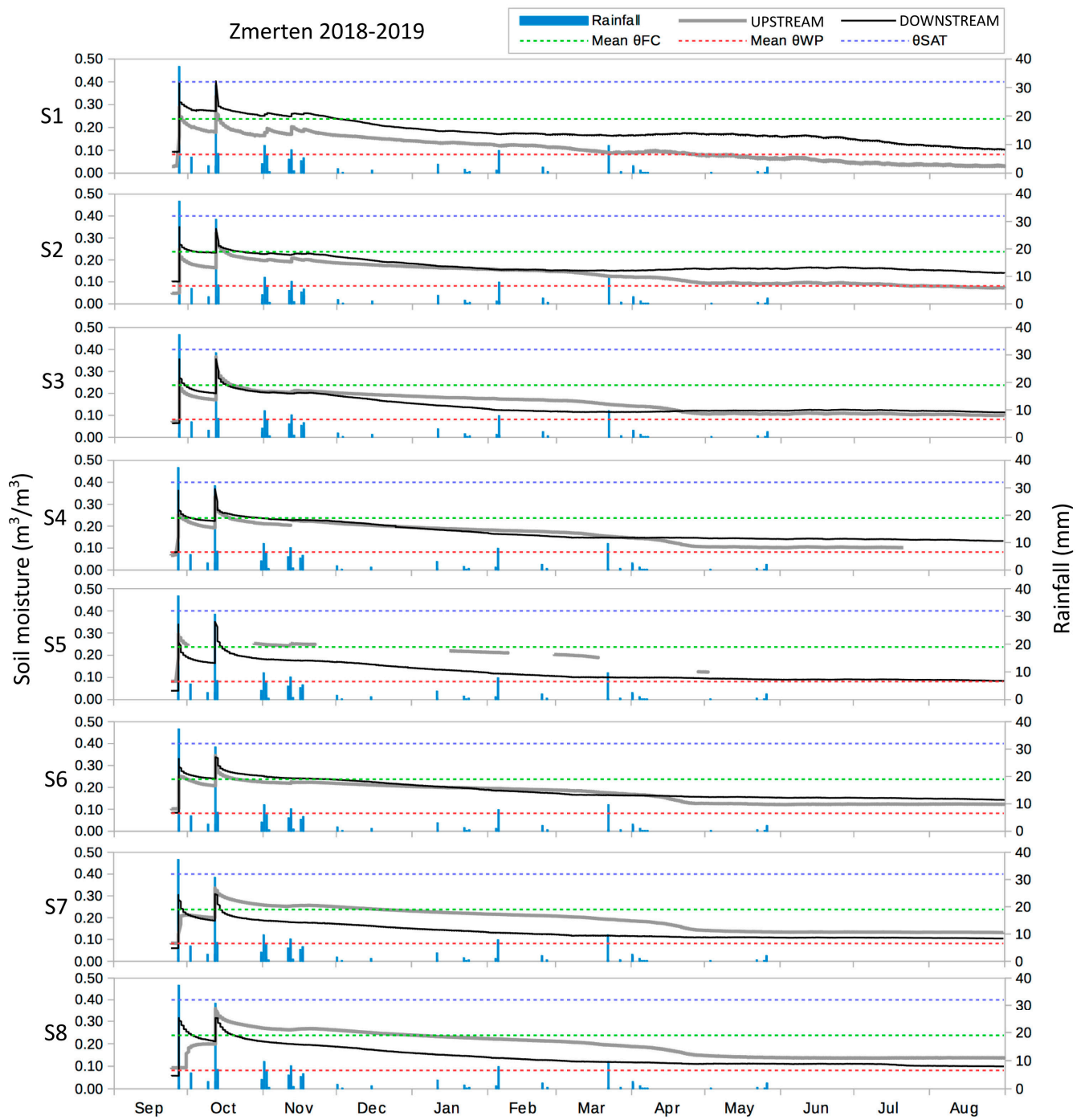


Figure 5. Evolution of soil moisture for the 8 sensors of upstream and downstream Jessour soil profiles (2018–19 agricultural year).

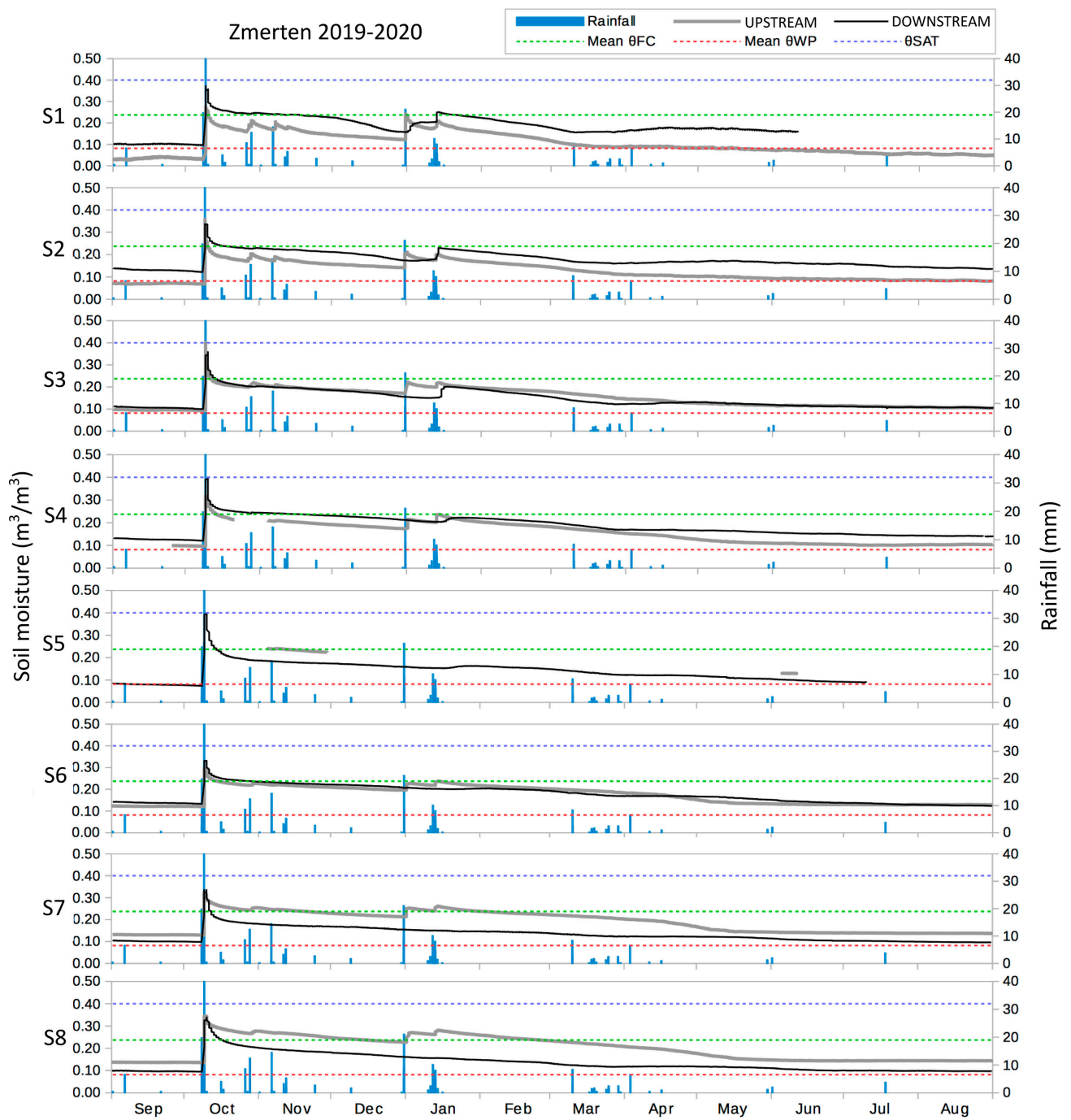


Figure 6. Evolution of soil moisture for the 8 sensors of upstream and downstream Jessour soil profiles (2019–20 agricultural year).

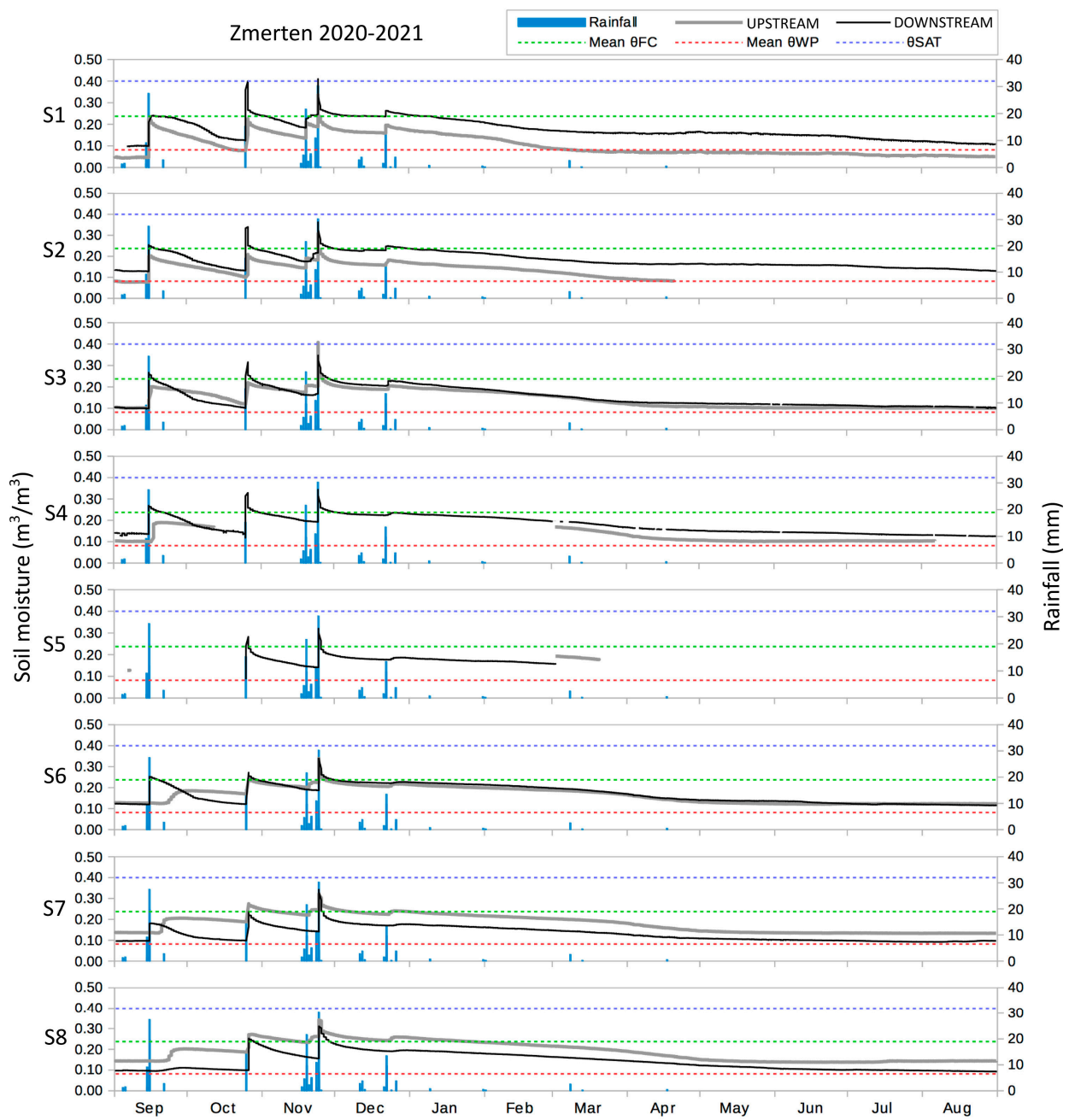


Figure 7. Evolution of soil moisture for the 8 sensors of upstream and downstream Jessour soil profiles (2020–21 agricultural year).

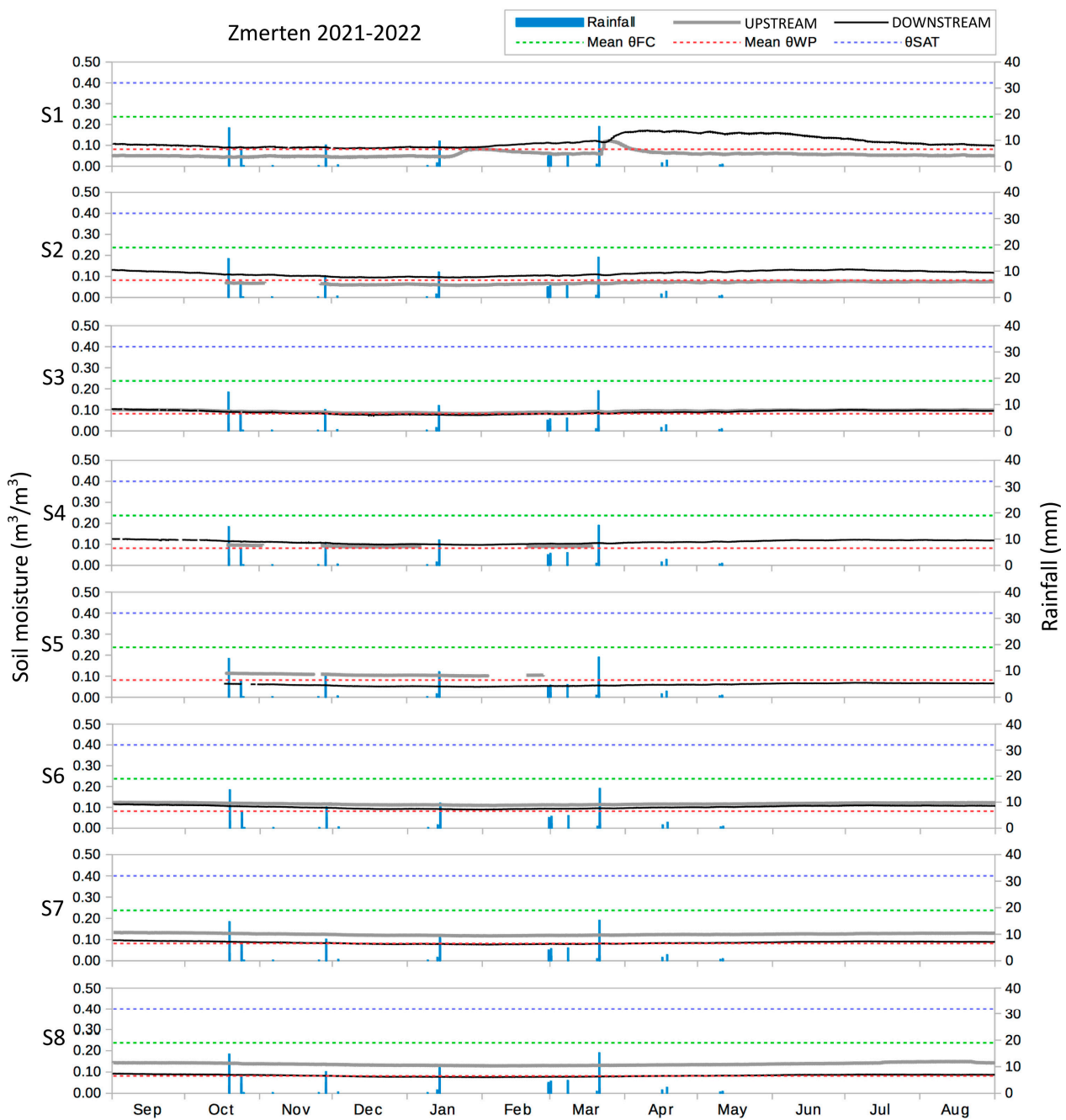


Figure 8. Evolution of soil moisture for the 8 sensors of upstream and downstream Jessour soil profiles (2021–22 agricultural year).

The soil moisture at saturation indicates that the surface of the terraces is saturated with water and that runoff is occurring in the Jessour system. We set the value of $0.40 \text{ m}^3/\text{m}^3$ for soil surface saturation in Zmertén. This is the value measured by the first sensor (S1, closest to the surface) in the upstream and downstream Jessour when a flooding of the terraces is observed in the field (see Figure 9).

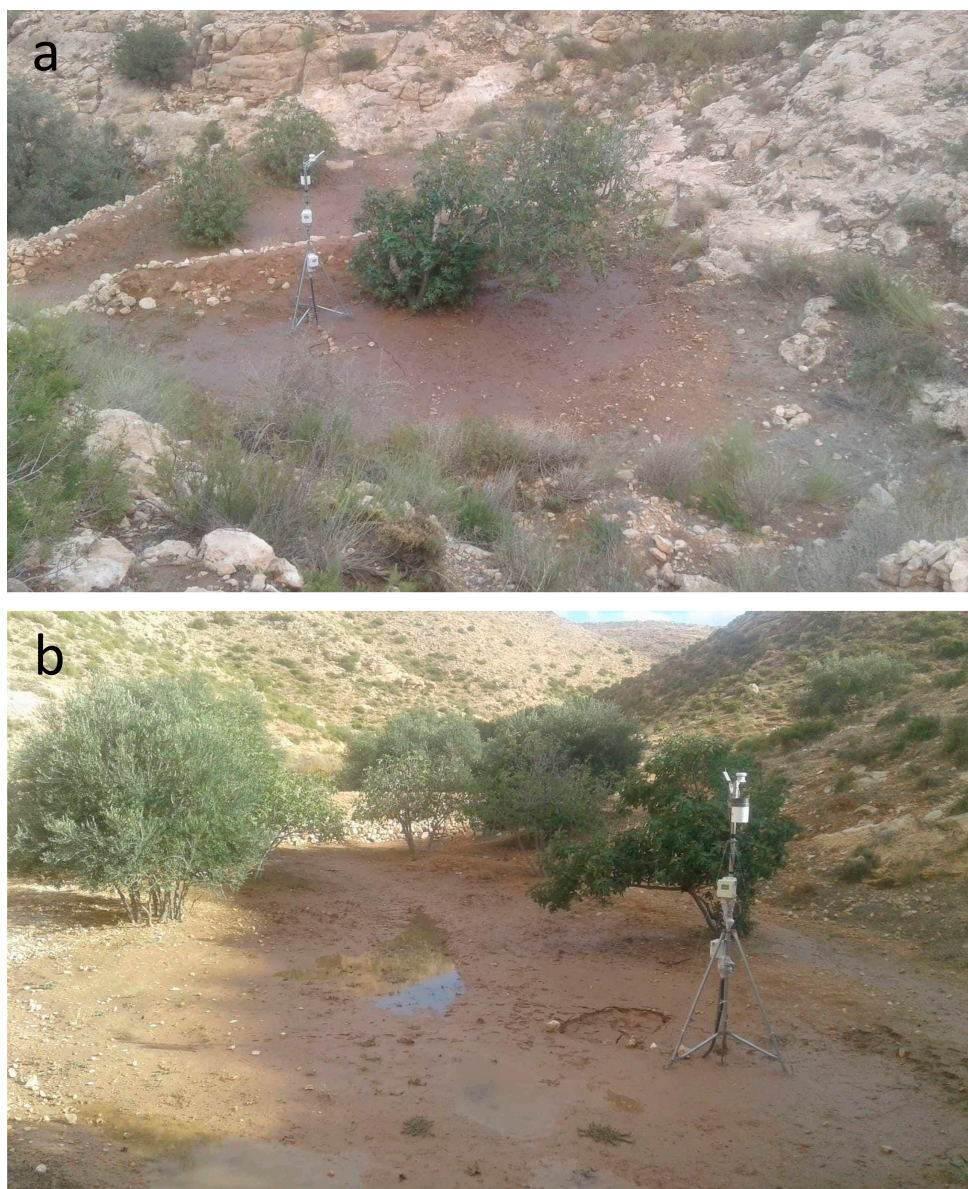


Figure 9. Upstream (a) and downstream (b) Jessour in Zmerten with the soil surface still saturated one day after the 27 September 2018 rainfall. Photos: M. Abbassi.

In the literature, the typical empirical value of soil moisture at saturation for a silt loam (as in Zmerten) is $0.48 \text{ m}^3/\text{m}^3$ [46]. In this work, the threshold value is lower because the first sensor gives a value representative of a soil layer that is a little deeper. S1 was located 20 cm below the surface and measured the water content in a 4.15 cm radius, i.e., from -15.85 cm to -24.15 cm . In addition, the soils in Zmerten have a high stone content so their porosity is lower than a “pure” silt loam and, therefore, become saturated at a lower water content.

When looking at the results without taking into account rainfall events, differences in soil moisture between sensors can already be observed. This is due to the soil texture and its organic matter content influencing the intrinsic ability of soils to retain water. In addition, the soil layers close to the surface (see sensors S1 and S2) are more sensitive to atmospheric conditions: they can be moistened by small rainfall events and they dry faster than deeper soils due to evaporation.

The 2018–19 agricultural year (Figure 5) was marked by two moderate autumnal rainfall events ($<35 \text{ mm}$) and was preceded by a very dry and hot summer: in late September

the majority of the sensors indicate soil moistures below the wilting point. In the upstream Jesr, the lowest values were near the surface ($S1 = 0.03 \text{ m}^3/\text{m}^3$ and $S2 = 0.05 \text{ m}^3/\text{m}^3$) and the highest values were at the bottom of the soil profile ($S6 = 0.10 \text{ m}^3/\text{m}^3$; $S7 = 0.08 \text{ m}^3/\text{m}^3$ and $S8 = 0.09 \text{ m}^3/\text{m}^3$). In the downstream Jesr, the surface layers were a little less dry ($S1 = 0.09 \text{ m}^3/\text{m}^3$ and $S2 = 0.10 \text{ m}^3/\text{m}^3$) than the bottom layers ($S6 = 0.08 \text{ m}^3/\text{m}^3$; $S7 = 0.06 \text{ m}^3/\text{m}^3$ and $S8 = 0.06 \text{ m}^3/\text{m}^3$). These differences in soil moistures, which stabilized after the dry season when the whole soil profile had dried out, highlight the effects of texture and organic matter content on soil moisture. The organic matter improves the coherence of the structural elements, promotes the retention of useful water and increases aeration of the soil [47]. The surface soil layer in the downstream Jesr contains more organic matter, is less sandy and contains fewer stones than the surface soil in the upstream Jesr so it better retains soil moisture. These values are similar to those found by Abdelli et al. [10] in Matmata, southeast Tunisia: “without effective rainfall during the first two years of measurement, [. . .] the water content in the surface layers, to a depth of 60 cm, remains below moisture at wilting point. The deeper horizons, have a moisture evolving between moisture at field capacity and soil moisture at the wilting point, with a higher water content in the horizons of depth beyond 1 m”.

The first autumnal rainfall (35 mm, on 27 September 2018) caused a peak of soil moisture above the field capacity for all sensors in the downstream Jesr. The values ranged from saturated soil moisture ($0.41 \text{ m}^3/\text{m}^3$) in the surface layer (S1) to $0.31 \text{ m}^3/\text{m}^3$ at a depth of 1.25 m (S8). Pounds formed in the upstream and the downstream Jessour which were flooded (Figure 9a,b). In the upstream Jesr, soil moisture peaks were also observed for the whole soil profile, but at a lower magnitude. The surface soil moisture was higher than the field capacity but it was not saturated ($S1 = 0.30 \text{ m}^3/\text{m}^3$), and a pound did not form in the upstream Jesr. Note that for the two deeper sensors, soil moisture peaks occurred a few days later after infiltration of the water column (1 day later for S7 and three days later for S8), and they had values below field capacity.

A second autumnal rainfall (33 mm, on 12 October 2018) occurred on soils that were still moist, leading to important soil moisture peaks affecting the entire soil profile and saturating the soil surface in both upstream and downstream Jessour, that certainly were flooded. The soil moisture ranged from $0.34 \text{ m}^3/\text{m}^3$ (S7) to $0.41 \text{ m}^3/\text{m}^3$ (S3) upstream and from $0.31 \text{ m}^3/\text{m}^3$ (S8) to $0.40 \text{ m}^3/\text{m}^3$ (S1) downstream.

In November, four rainfall events of less than 20 mm occurred. They only moistened the first 50 cm of the downstream Jesr (S1 to S3), whereas in the upstream Jesr, they moistened down to 80 cm (S1 to S5). The soil moisture peaks were small and did not reach values above $0.26 \text{ m}^3/\text{m}^3$.

During the two or three days following these autumnal rainfall events, the surface layers (S1 and S2) dried very quickly in the upstream Jesr and became the driest layers of the soil profile, whereas in the downstream Jesr, the surface layers dried out more slowly and remained the moistest layers until the next summer. The soil profiles then drained progressively during the dry season, until September the following year. At the end of the agricultural year (31 August 2019), the first 35 cm of soil in the upstream Jesr dropped below the wilting point ($S1 = 0.03 \text{ m}^3/\text{m}^3$ and $S2 = 0.07 \text{ m}^3/\text{m}^3$). In the downstream Jesr, the only sensor with a value below wilting point was S5 ($0.08 \text{ m}^3/\text{m}^3$). The 2019 dry season was less severe than in 2018.

Both in upstream and downstream Jessour, the deepest horizons retained soil moisture values that are useful for plants for a long time. As Gruhier et al. [48] report: “Unlike surface moisture which is experiencing strong variations (precipitation, rapid evaporation...), moisture of the deep root zone is that really used by vegetation. So the moisture throughout the root zone that has a real impact on exchanges soil-plant-atmosphere [49]”.

The 2019–20 agricultural year (Figure 6) was marked by an important autumnal rainfall event (105 mm, from 8 to 9 October 2019) that moistened the whole soil profiles of both the upstream and downstream Jessour. The soil moisture values exceeded values at field capacity for all the sensors, and the surface soils were saturated in the upstream and downstream Jessour, where runoff certainly occurred. As for the previous autumn, in

the upstream Jesr, the first 35 cm of soil (S1 and S2) showed the most intense drying rate, whereas in the downstream Jesr, S1 and S2 dried out less rapidly.

In October and November, four rainfall events below 16 mm impacted the soil profile upstream, but not downstream. Later, two more important rainfall events (40 mm on 31 December 2019 and 41 mm on 12–13 January 2020) moistened the entire upstream soil profile, but only the first 45 cm in the downstream profile (S1 to S3). After these rainfall events, only a few soil layers exceeded the field capacity: the two deepest sensors in the upstream Jesr and the surface sensor in the downstream Jesr.

During the dry season that followed (February–September 2020), the drainage was similar to the previous year, with an intense drying of the surface layers in the upstream Jesr and a better moisture retention in the downstream Jesr. At the end of the dry season (on 14 September 2020), the first 35 cm of soil in the upstream Jesr dropped below the wilting point ($S1 = 0.04 \text{ m}^3/\text{m}^3$ and $S2 = 0.08 \text{ m}^3/\text{m}^3$). In the downstream Jesr, the whole soil profile remained above the wilting point, with the lowest values observed in deep layers ($0.10 \text{ m}^3/\text{m}^3$ for S7 and S8).

The 2020–21 agricultural year (Figure 7) was marked by three important rainfall events and two moderate ones. The season started with a significant rainfall event at the beginning of the autumn (67 mm on 15 September 2020) that moistened the first 50 cm of soil in the upstream Jesr and the first 110 cm in the downstream Jesr. Upstream, soil moisture peaks appeared gradually for the deepest layers during the following days as the soil moisture column drained. Water transfer could also be seen downstream, with the moistening of the deepest layer (S8) starting about one week after rainfall. Maximum soil moisture values only slightly exceeded the wilting point downstream (with a maximum of $0.27 \text{ m}^3/\text{m}^3$ for S4, the moistest sensor before rainfall) and remained below the wilting point upstream (with a maximum of $0.23 \text{ m}^3/\text{m}^3$ for S1). An important drainage followed this early event: one month later, the first 50 cm of soil (S1 to S3) dropped back to soil moisture values similar to those observed at the end of the dry season.

On 25 October 2020, a small but very intense rainfall event (14 mm in 1 h) led to soil moisture peaks for all sensors, both in the upstream and downstream Jessour. Upstream, only three sensors showed values above field capacity. The maximum soil moisture value was $0.27 \text{ m}^3/\text{m}^3$ for the two deepest layers (S7 and S8), which remained the moistest layers after the previous rainfall. Downstream, all sensors showed values above field capacity and the surface layer (S1) exceeded $0.40 \text{ m}^3/\text{m}^3$, indicating a flooding of the terrace.

From 23 to 24 November 2020, a significant rainfall event (50 mm) moistened the whole soil profile of both the upstream and downstream Jesr. At that time, the soils were still moist from the 25 October rainfall and from a preceding rainy week (with for instance, a 36 mm rainfall on 18–19 November). This time, the surface sensor (S1) exceeded $0.40 \text{ m}^3/\text{m}^3$ at both sites, indicating runoff upstream and downstream.

Finally, on 22 December 2020, a 36 mm rainfall event provoked small soil moisture peaks that barely exceeded the field capacity, but contributed to maintaining high values of soil moisture at both sites, constituting important water storage for the dry season.

The 2021–22 agricultural year (Figure 8) was marked by very significant dryness. Rainfall events occurred in autumn, but they were all below 18 mm. There was almost no effective rainfall. The soil moisture values remained well below the field capacity and small peaks occurred only for the shallowest soil layer (S1) in upstream and downstream Jessour. The values slightly rose from 0.05 to $0.08 \text{ m}^3/\text{m}^3$ (only upstream and for S1) after the 26 mm rainfall of 14 January 2022. Soil moisture barely rose to $0.16 \text{ m}^3/\text{m}^3$ downstream (for S1 only) and to $0.12 \text{ m}^3/\text{m}^3$ upstream (for S1 only) after the 26 mm rainfall of 21 March 2022. Upstream, the moistest layers were at depth while downstream, the moistest layers were at the surface. This shows that the root system of the plantations downstream maintains a little moisture on the surface.

3.4. Capacity of Upstream and Downstream Jessour to Retain Available Water Content

In this section we focus on the ability of the upstream and downstream Jessour to maintain soil water storage from the autumnal rainfall events until and through the dry season. The analysis is based on the evolution of available water content (AWC) in the whole 1.25 m soil profile and evapotranspiration (ET₀) (Figure 10). The theoretical maximum AWC, based on soil texture and organic matter content, is 197 mm in the upstream Jesr and 203 mm in the downstream Jesr.

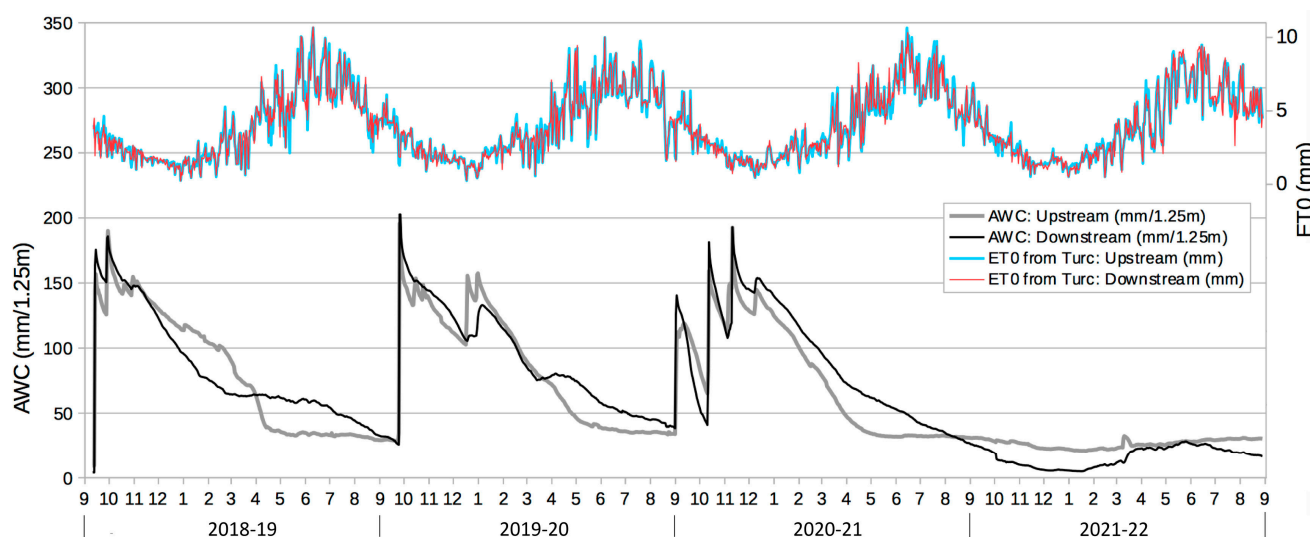


Figure 10. Evolution of available water content (AWC) in upstream and downstream Jessour soil profiles and evapotranspiration (ET₀).

3.5. Agricultural Year 2018–19

At the end of the dry season (26 September 2018), the available water content was very low: 9 mm in the upstream Jesr and 4 mm in the downstream Jesr. After the first autumnal rainfall (28 September 2018), the AWC increased to 157 mm upstream and 176 mm downstream. During the two following weeks, the upstream Jesr drained much faster than the downstream Jesr. The drainage rates were -1.98 mm/day (upstream) and -1.51 mm/day (downstream).

After the second autumnal rainfall event (13 October 2018), the AWC increased again to 190 mm (upstream) and 186 mm (downstream). During the following dry period (14–31 October 2018), the upstream Jesr also showed the highest drainage rate, with -2.17 mm/day compared with -1.44 mm/day downstream. Then, between the end of the rainy season and the rise in evapotranspiration (from 14 November 2018 to 27 February 2019), the drainage was more significant in the downstream Jesr. On average during this period, the drainage was -0.46 mm/day upstream and -0.81 mm/day downstream. On 20 February 2019, before spring, the upstream Jesr contained more AWC (103 mm) than the downstream Jesr (74 mm) (Table 4). However, during the spring period (from 3 March to 26 April 2019), the situation reversed: the drainage almost stopped in the downstream Jesr, which stabilized at an average of -0.04 mm/day, whereas there was a slope break for the upstream Jesr, draining even faster than before spring at an average of -1.01 mm/day. This intense drainage upstream corresponded to the first peak of ET₀ above 7 mm/day.

Table 4. AWC (mm) at three specific times of the agricultural year in the upstream and downstream Jessour.

Date	Jesr	AWC (mm) Agricultural Year 2018–2019	AWC (mm) Agricultural Year 2019–2020	AWC (mm) Agricultural Year 2020–2021	AWC (mm) Agricultural Year 2021–2022
20 February	Upstream	103	115	93	22
	Downstream	74	111	111	9
15 June	Upstream	35	38	32	28
	Downstream	61	56	57	26
End of dry season	Upstream	28 (7 October)	33 (14 September)	32 (1 October)	29 (18 October)
	Downstream	26 (7 October)	38 (14 September)	25 (1 October)	14 (18 October)

During the driest and hottest period (May to August) when plants water needs are the highest, the AWC values were stable both upstream and downstream, but the downstream Jesr provided higher water content. On 15 June 2019, when ET₀ was at maximum (above 10 mm/day), the downstream Jesr contained 61 mm of AWC and the upstream Jesr 35 mm. Then, from August to the end of the dry season (October), the downstream Jesr started to drain again, whereas the upstream Jesr remained almost steady. On 7 October 2019, there was 28 mm available upstream and 26 mm downstream.

3.6. Agricultural Year 2019–20

The first autumnal rainfall event of 9 October 2019 provoked an important rise in AWC both upstream (196 mm) and downstream (203 mm). Right after this rainfall event, as during the previous season, the upstream Jesr drained much faster than the downstream Jesr, but thanks to small recharges of the upstream Jesr after moderate rainfall events in late October and early November, the average drainage rate from October to December was similar upstream (−0.70 mm/day) and downstream (−0.79 mm/day). On 30 December 2019, the AWC values were lower than for the same period of the previous year and similar at both sites: 103 mm upstream and 106 mm downstream.

The humid season lasted longer than the previous year: after the two moderate rainfalls on 13 December 2019 and 12–13 January 2020, the AWC values rose again upstream (157 mm) and downstream (133 mm). On 20 February 2020, before spring, the upstream Jesr contained almost as much AWC (115 mm) as the downstream Jesr (111 mm) (Table 4). These values were higher than in 2019 at the same date (103 and 74 mm respectively). From that day until 14 April 2020, the drainage was more significant upstream (−0.81 mm/day) than downstream (−0.67 mm/day). Starting from 15 April, there was an AWC slope break for the upstream Jesr, which dried much faster than the downstream Jesr. Until 31 May 2020, the upstream Jesr drained at a rate of −0.70 mm/day and the downstream Jesr at a rate of −0.30 mm/day. As in 2019, this more intense drainage upstream corresponded to the first peak of ET₀ above 7 mm/day. On 15 June 2020, when ET₀ was at a maximum (10 mm/day), the downstream Jesr contained more AWC (56 mm) than the upstream Jesr (38 mm). This pattern is almost identical to that of the previous year. At the end of the dry season (14 September 2020) the AWC decreased to 33 mm upstream and 38 mm downstream.

3.7. Agricultural Year 2020–21

After the early autumnal rainfall of 16 September 2020, the AWC reached 110 mm upstream and 140 mm downstream. This was followed by intense drainage, especially downstream: the AWC values dropped down to 41 mm, almost as dry as at the end of the drying season. The second rainfall event on 25 October 2020 more efficiently moistened both the upstream (AWC: 158 mm) and downstream Jesr (AWC: 181 mm). The rainfall events of late November also recharged the soils to up to 193 mm of AWC in both Jessour. From December,

the upstream Jesr drained more rapidly than the downstream Jesr, as in the previous years. On 21 December 2020, the AWC was 124 mm upstream and 142 mm downstream.

Then, the moderate rainfall of 22 December 2020 moistened both Jessour, but the upstream site remained drier (AWC: 142 mm) than downstream (AWC: 154 mm). Before spring, on 20 February 2021, the AWC reached 93 mm upstream and 111 mm downstream. On 14 May 2020, when ET₀ peaks started to exceed 7 mm/day, the downstream AWC (66 mm) was twice as high as the upstream AWC (34 mm). One month later, on 15 June 2020, the upstream AWC remained almost unchanged (32 mm), and the downstream Jesr still maintained an AWC of 57 mm. During the following months, the upstream AWC stayed constant around 32 mm, whereas the downstream AWC continued draining to reach 25 mm on 1 October 2021.

3.8. Agricultural Year 2021–22

During this particularly dry year, there was no significant recharge of AWC. The values did not exceed 32 mm upstream and 28 mm downstream. Since May 2021 of the previous agricultural year, the available water content stayed stable in the upstream Jesr (around 25 mm), while it was decreasing in the downstream Jesr until late autumn (until the minimum of evapotranspiration values), reaching values close to zero. From September 2021, the AWC was lower downstream than upstream. This could be attributed to the transpiration of the olive trees in the large downstream plot. From January 2022, the AWC increased and reached the values of the upstream thanks to the small rain events of March. In June, with the return of significant evapotranspiration, the AWC decreased again downstream, while it remained stable upstream.

3.9. Activation and Recharge of the Jessour According to Rainfall Typology

To identify threshold values representative of the Jessour system, we examined the relationships between the event cumulative rainfall, the rainfall event intensity (i.e., event cumulative rainfall divided by rain duration), the soil profile recharge and the activation of the Jessour (Figure 11).

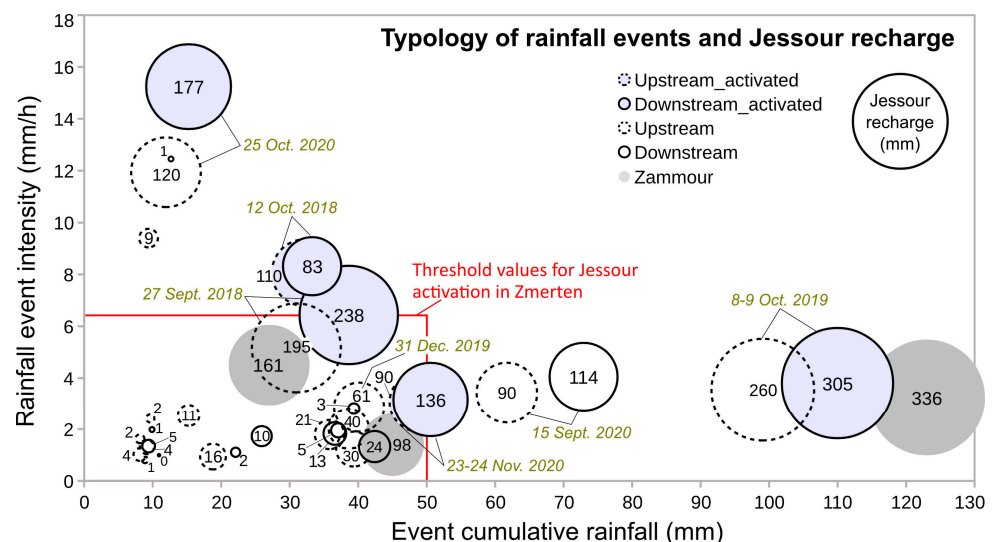


Figure 11. Typology of rainfall events (maximum hourly intensity, event cumulative rainfall), activation and soil moisture recharge for the upstream and downstream Jessour. The values in grey are for the site of Zammour, investigated with the same approach in a previous study [11].

From Zmerten’s data, events with a cumulative rainfall above 8 mm were selected (see Figure 11). Each “bubble” represents a rainfall event and is positioned in the chart according to its intensity and cumulative rainfall. The bubble size indicates the Jesr recharge. Events leading to activation are colored in blue. The results show that the Jessour system in

Zmertén is activated by rainfall events that can be of three types: (i) *High accumulation/low intensity* (causing saturation- excess runoff). Activation was observed both upstream and downstream from 50 mm of cumulative rainfall (event of 23–24 November 2020 with an intensity of 3.1 mm/h, on wet soils); (ii) *High intensity/low accumulation* (causing infiltration/excess runoff). Activation was observed downstream from an intensity of 15.2 mm/h (event of 25 October 2020 with cumulative rainfall of 15 mm, on relatively dry soils); (iii) *Combination of moderate intensity and moderate accumulation*. Activation was observed downstream from an intensity of 6.4 mm/h and a cumulative rainfall of 39 mm (event of 27 September 2018, on dry soils). Activation was observed both upstream and downstream from an intensity of 8 mm/h and a cumulative rainfall of 33 mm (event of 12 October 2018, on wet soils). From these results, we propose to set 50 mm of cumulative rainfall and/or 6.4 mm/h of intensity as threshold values for the activation of the Jessour system in Zmertén (see black rectangle in Figure 11).

An interesting result is that significant soil moisture recharges can occur even without activation of the Jessour system. Low intensity events with moderate cumulative rainfall are able to efficiently recharge soil profiles. This can be the case of events occurring at the beginning of the rainy season, on dry soil, where saturation/excess runoff does not occur but where the infiltration is significant. The recharge can also be supplied by lateral and longitudinal underflows. Examples are: the recharge of 61 mm (upstream Jesr) with 40 mm of cumulative rainfall and 2.9 mm/h of intensity on 31 December 2019; and the recharge of 90 mm (upstream Jesr) and 114 mm (downstream Jesr) with 67 mm of cumulative rainfall and 3.7 mm/h of intensity on 15 September 2020.

Furthermore, the sequence of rainfall events plays an important role in the response of soil profiles. Successive moderate rainfall events maintain soil moisture and favor runoff, as soils saturate more rapidly. For instance, the highest soil moisture was observed in the downstream Jesr ($0.41 \text{ m}^3/\text{m}^3$) after the consecutive moderate rains of November 2020, rather than after the most intense rainfall episodes. Conversely, a rainfall event occurring on a dry soil profile will maximize its recharge. Finally, the period of the year also plays an important role. The first rainfall events occurring at the end of the summer period when the soils are very dry are able to infiltrate the entire rainfall volume. For instance, the event of 15 September 2020, despite relatively high intensities (3.4 mm/h upstream and 4.1 mm downstream) and accumulations (62 mm upstream, 73 mm downstream) did not activate the Jessour, but allowed a significant recharge. However, as this event occurred very early, when the summer period was not over and the evapotranspiration was still high, it was followed by a rapid drying of the soil profile (see Figure 10). In the end, such early events are not profitable for the crops, as the soils will not store enough water until the dry season. Rainfall events occurring from October onwards, when temperature and evapotranspiration decrease, are more likely to generate a water storage that will last until the following dry season.

3.10. Comparison with the Site of Zammour

This study follows another one carried out in Zammour (20 km south of Zmertén; see Figure 1), where a Jesr was instrumented during one year (from October 2017 to October 2018) using the same methodology [11]. During this period, the Jesr in Zammour experienced three rainfall events leading to significant recharges of the soil profile (see the grey bubbles in Figure 11). The first event, from 10 to 12 November 2017, was a high cumulative rainfall with moderate intensity (123 mm in 38 h, i.e., 3.24 mm/h). It did not saturate the surface soils ($S_1 = 0.34 \text{ m}^3/\text{m}^3$), but all the sensors peaked above the field capacity (to 1.25 m deep). The Jesr reached the theoretical maximum AWC (116.2 mm), and the recharge was very significant (336 mm). The second event, from 20 to 21 December 2017, was a moderate cumulative rainfall with low intensity, but on previously moistened soils (45 mm in 32 h, i.e., 1.44 mm/h). It did not saturate the surface soils ($S_1 = 0.28 \text{ m}^3/\text{m}^3$), but all the sensors peaked above the field capacity. The AWC in the Jesr was not influenced

by the rainfall event, as the soils were still sufficiently moist to ensure full available water storage. The recharge was lower for that reason (98 mm).

The third event was a summer thunderstorm on 19 August 2018, with moderate cumulative rainfall but quite high intensity (26.7 mm in 6 h, i.e., 4.45 mm/h). As for the other events, it did not saturate the surface soils ($S1 = 0.27 \text{ m}^3/\text{m}^3$) but all sensors peaked above the field capacity. The recharge was 161 mm.

Because soils in Zammour are sandier than those in Zmerten ([11], see Table 2), the maximum available water content and the soil moisture at saturation are lower. However, sandy soils have a higher infiltration capacity which can explain the significant recharge values (see Figure 11), even with rainfall events that did not activate the Jessour system. According to cumulative rainfall and intensity, the recharges in Zammour are similar to those in Zmerten. But differences are observed during the drainage period. In Zammour, the Jesr maintained the soil moisture longer after the rainy season and through the dry season than in Zmerten. The AWC remained at its maximum threshold value (116 mm) from November to March, then decreased to stabilize at around 60 mm in July. Water conservation may be favored in Zammour due to its gentle slope (limiting drainage by underflows), its larger terrace and deeper sediment deposits (favoring water accumulation).

4. Discussion

4.1. Similarities and Differences between the Upstream and Downstream Jessour

When runoff and flooding occur in the Jessour system, the entire soil profiles in both upstream and downstream Jesr are moistened, and AWC peaks are observed for all sensors. The upstream Jesr appears to be more sensitive to small rainfall events without runoff. For the four measured autumnal seasons, the total recharge values (increases of AWC from initial “dry” values until peak values after rainfall events) are very similar in the downstream Jesr (1080 mm) and in the upstream Jesr (1104 mm). In addition, for the four years, total drainage values (decrease in AWC from a peak value to the value before the next rainfall) were almost identical: -1046 mm upstream and -1066 mm downstream. However, what should be noted are the values of AWC during the most critical period for the vegetation, i.e., the arid summer (from June to August). At that time of highest plant water needs, the AWC is systematically higher (nearly twice as high) in the downstream Jesr than in the upstream Jesr (Table 4). We also observed that the downstream Jesr was activated more often than the upstream Jesr. This highlights the advantage of being located downstream in the Jessour system, with the benefits of the runoff coming from the entire impluvium overflowing from the series of upstream Jessour. Moreover, the downstream Jessour benefits more from the subsurface flow [11], whose water contribution would be more important than for the upstream Jessour since the value of the slope near the upstream Jessour of the Dahar Waja gully reaches 29%, but it is only 6% near the downstream Jessour. As the downstream Jesr is deeper and larger, it also provides more inertia thanks to the larger volume of sediment.

Observations in Zmerten show that “extreme events”, with very intense rainfall (e.g., more than 12 mm/h on 25 October 2020) or with high cumulative volumes (e.g., more than 99 mm on 8–9 October 2019) only lead to the activation of the downstream Jesr (see Figure 11).

Another particularity of the downstream Jesr is that during dry years, its surface soil remains moister than that in the upstream Jesr thanks to its trees providing shade and humidity for the root systems. This also points out the importance of continuous measurements (or measuring at the right periods) rather than annual water balances.

4.2. Comparison with Similar Water Harvesting Techniques

The fact that lower areas in terrace systems are more moist was already documented [20]. In the case of bench terraces, it is shown that wide terraces retain more water on a percentage basis than narrow ones due to a lower evaporating surface area per unit volume of water storage [50]. This is the case in Zmerten, where the upstream terrace is about 6 times smaller than the downstream terrace and the impluvium ten times smaller. Differences

in soil moisture can also be due to terrace orientation, for instance between the northern and southern slopes [51]. This factor is irrelevant in Zmertem as both Jessour present the same orientation. Moreover, agricultural practices can play a role in soil moisture, for instance, the cropping density (which influences the soil organic matter content and root absorption capacity) and tillage techniques. The absorption capacity of different crop roots is an important factor influencing the dynamic changes in soil moisture [52]. As the downstream Jessour contains more trees and more intercropping, on one side, the vegetation consumes more soil water, but on the other side, the root systems favor infiltration and provide soil organic matter, which improve soil moisture retention. The tillage performed for intercropping in the spaces between the Jessour's trees also favors infiltration [53], and the intercropping area is higher in the downstream Jessour.

Considering the capacity of water harvesting terraces to retain and store soil moisture, similar results were found in a wadi basin in Egypt using a monitoring-modeling approach [54]. In this case study, the soil profile in terraces was able to retain about 40% of the initial volume, and most of the water stored could be used by crops during the whole spring–summer period.

4.3. Dynamics of Available Water Content and Olive Tree Vegetative Cycle

Considering the interaction between crops and soil water storage, the AWC dynamics can be compared with the olive tree vegetative cycle (i.e., the times of water needs) which in Mediterranean climates, corresponds to two periods: from March to June, during the spring awakening and flowering, and from September to October, during the autumnal vegetative development, when the olive fruits are growing [11,55]. It is exactly during these two periods that the downstream Jessour maintains a steady storage of available water content, whereas the upstream Jessour continues to drain. In the summer period (July–August), the vegetative growth is paused, and the olive trees reduce transpiration as an adaptation to the hot and dry conditions. During the 2021–2022 dry year, the little remaining available water content in the downstream Jessour was used for the transpiration of olive trees during the autumnal vegetative development. Upstream, the AWC remained stable.

5. Conclusions

Weather parameters (temperature, solar radiation, rainfall) and soil moisture profiles (eight sensors, placed every 15 cm in a 1.25 m deep trench) were measured at hourly time steps during four agricultural years (September to October) (2018–19 to 2021–22) in two water harvesting terraces (Jessour) of the same valley near the village of Zmertem (southeastern Tunisia), a region characterized by an arid climate. The first instrumented Jessour was located in the upstream section of the valley and the other in the downstream section. The objectives of this work were to evaluate the differences in terms of soil moisture dynamics (recharge during the rainy season and retention during the dry season) in the upstream and downstream sections of the Jessour system and to determine the precipitation thresholds from which the Jessour system is activated (i.e., runoff is triggered and the Jessour are overflowing into one another). The soil profiles are dominated by a silt loam structure, but the upstream Jessour contains coarser elements ranging from the size of gravel to small blocks (diameter: 10 cm) of limestone and dolomite.

From the meteorological point of view, we were able to observe four different types of year: 2018–19 with two autumnal rains recharging the Jessour; 2019–20 with one autumnal rain recharging the Jessour and two moderate rains in winter; 2020–21 with a very early autumnal rain recharging both Jessour but followed by intense drying and a succession of three recharging rains until December; and, finally, a very dry 2021–22 year.

The comparison between the upstream and downstream Jessour showed that every year, the downstream Jessour had higher available water content than the upstream Jessour, during the dry period from April until the first significant rains of autumn. During this period, when crops are under stress from the summer dry and hot conditions, the downstream Jessour maintained the entire soil profile above the wilting point, whereas the moisture measured

by the two surface sensors in the upstream Jesr fell below the wilting point. During the very dry 2021–22 agricultural year, the little available water that remained in the downstream Jesr could be used by the olive trees. Moreover, the downstream Jesr, which benefits from the runoff coming from the whole terrace system, was activated more often than the upstream Jesr. When the autumn was rainy, at least one rainfall event activated the upstream Jessour. In winter (January–March) the situation varied from year to year. The upstream Jesr was more sensitive to light rains as its surface layers could be moistened, which was not the case downstream. This allowed small recharges of the upstream Jesr in spring, which helped to slow down the drying of the profile compared with the downstream profile. In addition to the fact that the downstream Jesr benefits from a larger impluvium and from the water overflow from upstream Jessour, the higher capacity of the downstream Jesr to maintain soil water storage might also come from its larger dimensions (terrace soil depth and surface) providing more inertia. The cultivable plots in the larger Jessour that hold the moisture in the surface layers longer have an advantage for the cultivation of cereals and leguminous plants with a superficial root system.

The rainfall typology showed that high accumulation/low intensity rainfalls (causing saturation/excess runoff) activated both upstream and downstream Jessour from 50 mm of cumulative rainfall (with an intensity of 3.1 mm/h on wet soils). It was also observed that high intensity/low accumulation rainfalls (causing infiltration/excess runoff) activated the downstream Jesr from an intensity of 15.2 mm/h (with cumulative rainfall of 15 mm, on relatively dry soils). Finally, a combination of moderate intensity and moderate accumulation rainfalls activated the downstream Jesr from an intensity of 6.4 mm/h and a cumulative rainfall of 39 mm (on dry soils) and activated both upstream and downstream Jessour from an intensity of 8 mm/h and a cumulative rainfall of 33 mm (on wet soils). We propose to set 50 mm of cumulative rainfall and/or 6.4 mm/h of intensity as threshold values for the activation of the Jessour system in Zmertén. An initially wet soil is also a factor favoring the activation. Yet, significant soil moisture recharges can occur even without activation of the Jessour system. The ability of a rainfall event to recharge the Jessour soils is favored by an initially dry soil, a high infiltration capacity, a large volume of sediments and a gentle slope. The ability of the Jessour system to retain soil moisture from autumnal rainfalls until the next dry season is favored by a high amount of soil organic matter, the presence of vegetation root systems, a low evapotranspiration after rainfall events, a large volume of sediments and a gentle slope. Water content is effectively maintained when rainfall events occur from October to January, as the evapotranspiration is lower.

More generally, this study confirms the importance of Jessour for water conservation, as highlighted by previous studies in the region [6,9,11,14] and adds threshold values to complement recent quantitative works [10,12,21,22], helping to understand the dynamics of these systems of terraces that allow agriculture in arid conditions.

Author Contributions: Conceptualization, M.C., T.B.F., J.-M.F., H.B.O. and E.R.; Data curation, M.C. and T.B.F.; Formal analysis, M.C. and T.B.F.; Funding acquisition, H.B.O. and E.R.; Field investigation, M.A., M.C., T.B.F., A.G.M., H.B.O., J.-M.F. and E.R.; Methodology, M.C., J.-M.F., T.B.F. and A.G.M.; Project administration, H.B.O. and E.R.; Writing—original draft, M.C.; Writing—review and editing, E.R., T.B.F., J.-M.F., A.G.M. and H.B.O. All authors have read and agreed to the published version of the manuscript.

Funding: The measurement stations were provided by the Investment Fund of the Faculty of Geosciences and Environment (FGSE) of Lausanne University. The fieldwork costs were paid by the Institute of Geography and Sustainability (IGD) of Lausanne University and by the Laboratory of Geomorphologic Cartography of Settings, Environments and Dynamics (CGMED) of Tunis University. The analysis of data and writing of the paper was funded by a special grant of the Institute of Geography and Sustainability (IGD) of Lausanne University.

Data Availability Statement: Publicly available datasets were analyzed in this study. This data can be found here: [https://www.dropbox.com/s/gzgagm6vo7k0bio/Zmertene_2018_21.ods?dl=0] (accessed on 12 February 2023).

Acknowledgments: The sedimentological analyses were performed at the Sedimentology Laboratory of the Institute of Earth Sciences (ISTE) of Lausanne University, run by Thierry Adatte, who is acknowledged for his help. We thank Ali Bou Hela owner of the “Zmertén guest house” who contributed to the maintenance and surveillance of the equipment during the measurement periods and the field owner, Amor Ben Slimene, for allowing us to install the equipment in his field. We are grateful to the two anonymous reviewers for their useful comments which helped us to improve the original manuscript.

Conflicts of Interest: The authors declare no conflict of interest.

References

- Mwenge Kahinda, J.; Taigbenu, A.E. Rainwater Harvesting in South Africa: Challenges and Opportunities. *Phys. Chem. Earth Parts A/B/C* **2011**, *36*, 968–976. [[CrossRef](#)]
- Bonvallot, J. Comportement Des Ouvrages de Petite Hydraulique Dans La Région de Médenine (Tunisie Du Sud) Au Cours Des Pluies Exceptionnelles de Mars 1979. *Cah. ORSTOM Sci. Hum.* **1979**, *16*, 233–249.
- Abdelli, F.; Ouessar, M.; Khatteli, H. Méthodologie d’identification Des Ouvrages Existants et Des Sites Potentiels Pour Les Jessour. *Rev. Des Sci. De L’eau/J. Water Sci.* **2012**, *25*, 237–254. [[CrossRef](#)]
- Al-Seekh, S.H.; Mohammad, A.G. The Effect of Water Harvesting Techniques on Runoff, Sedimentation, and Soil Properties. *Environ. Manag.* **2009**, *44*, 37–45. [[CrossRef](#)]
- Ben Fraj, T.; Abderrahmen, A.; Ben Ouedzou, H.; Reynard, E.; Milano, M.; Calianno, M.; Fallot, J.-M. Les Jessour Dans Le Sud-Est Tunisien: Un Système Hydro-Agricole Ancestral Dans Un Milieu Aride. In Proceedings of the Actes du 29ème Colloque de l’Association Internationale de Climatologie (AIC), Lausanne, Switzerland, 6–9 September 2016; pp. 193–198.
- Gasmi, I.; Eslamian, S.; Moussa, M. Evaluation of Traditional Rainwater Harvesting Technique of “Jessour” in Southern Tunisia, a Case Study on El-Jouabit Catchment. In *Handbook of Water Harvesting and Conservation*; Eslamian, S., Eslamian, F., Eds.; John Wiley & Sons, Ltd: Chichester, UK, 2021; pp. 199–212. ISBN 978-1-119-77601-7.
- Abderrahmen, A. Les Intensités Des Pluies Dans La Tunisie Orientale. Ph.D. Thesis, Faculté des Sciences Humaines et Sociales de Tunis, Tunis, Tunisia, 2009.
- Bresci, E.; Castelli, G. Water Harvesting in Farmlands. In *Handbook of Water Harvesting and Conservation*; Eslamian, S., Ed.; Wiley: New York, NY, USA, 2021; pp. 87–100, ISBN 978-1-119-47891-1.
- Piras, F.; Zanzana, A.; Costa Pinto, L.M.; Fiore, B.; Venturi, M. The Role of the Jessour System for Agrobiodiversity Preservation in Southern Tunisia. *Biodivers. Conserv.* **2021**, *31*, 2479–2494. [[CrossRef](#)]
- Abdelli, F.; Ouessar, M.; M’Hemdi, S.; Guied, M.; Khatteli, H. Monitoring Soil Moisture Content of Jessour in the Watershed of Wadi Jir (Matmata, Southeast Tunisia). In *Water and Land Security in Drylands*; Ouessar, M., Gabriels, D., Tsunekawa, A., Evett, S., Eds.; Springer International Publishing: Cham, Switzerland, 2017; pp. 97–110, ISBN 978-3-319-54020-7.
- Calianno, M.; Fallot, J.-M.; Ben Fraj, T.; Ben Ouedzou, H.; Reynard, E.; Milano, M.; Abbassi, M.; Ghram Messedi, A.; Adatte, T. Benefits of Water-Harvesting Systems (Jessour) on Soil Water Retention in Southeast Tunisia. *Water* **2020**, *12*, 295. [[CrossRef](#)]
- Ouessar, M.; Bruggeman, A.; Abdelli, F.; Mohtar, R.H.; Gabriels, D.; Cornelis, W.M. Modelling Water-Harvesting Systems in the Arid South of Tunisia Using SWAT. *Hydrol. Earth Syst. Sci.* **2009**, *13*, 2003–2021. [[CrossRef](#)]
- Jothiprakash, V.; Sathe, M.V. Evaluation of Rainwater Harvesting Methods and Structures Using Analytical Hierarchy Process for a Large Scale Industrial Area. *J. Water Resour. Prot.* **2009**, *1*, 427–438. [[CrossRef](#)]
- Adham, A.; Riksen, M.; Ouessar, M.; Ritsema, C. A Methodology to Assess and Evaluate Rainwater Harvesting Techniques in (Semi-) Arid Regions. *Water* **2016**, *8*, 198. [[CrossRef](#)]
- Grum, B.; Woldearegay, K.; Hessel, R.; Baartman, J.E.M.; Abdulkadir, M.; Yazew, E.; Kessler, A.; Ritsema, C.J.; Geissen, V. Assessing the Effect of Water Harvesting Techniques on Event-Based Hydrological Responses and Sediment Yield at a Catchment Scale in Northern Ethiopia Using the Limburg Soil Erosion Model (LISEM). *CATENA* **2017**, *159*, 20–34. [[CrossRef](#)]
- Carletti, A.; Canu, S.; Motroni, A.; Ghiglieri, G. A Combined Methodology for Estimating the Potential Natural Aquifer Recharge in an Arid Environment. *Hydrol. Sci. J.* **2019**, *64*, 1727–1745. [[CrossRef](#)]
- Fleskens, L.; Stroosnijder, L.; Ouessar, M.; De Graaff, J. Evaluation of the On-Site Impact of Water Harvesting in Southern Tunisia. *J. Arid. Environ.* **2005**, *62*, 613–630. [[CrossRef](#)]
- Tadros, M.J.; Al-Mefleh, N.K.; Othman, Y.A.; Al-Assaf, A. Water Harvesting Techniques for Improving Soil Water Content, and Morpho-Physiology of Pistachio Trees under Rainfed Conditions. *Agric. Water Manage.* **2021**, *243*, 106464. [[CrossRef](#)]
- Saeed, A.B.; Hamid, A.M.N.; Abdalhi, M.A.M.; Mohamed, A.A. Evaluation the Effects of Water Harvesting Techniques in Improving Water Conservation and Increasing Crop Yields. *Int. J. Sci. Eng. Investig.* **2019**, *8*, 9.
- Mesfin, S.; Almeida Oliveira, L.A.; Yazew, E.; Bresci, E.; Castelli, G. Spatial Variability of Soil Moisture in Newly Implemented Agricultural Bench Terraces in the Ethiopian Plateau. *Water* **2019**, *11*, 2134. [[CrossRef](#)]
- Schiettecatte, W.; Ouessar, M.; Gabriels, D.; Tanghe, S.; Heirman, S.; Abdelli, F. Impact of Water Harvesting Techniques on Soil and Water Conservation: A Case Study on a Micro Catchment in Southeastern Tunisia. *J. Arid. Environ.* **2005**, *61*, 297–313. [[CrossRef](#)]
- Castelli, G.; Oliveira, L.A.A.; Abdelli, F.; Dhaou, H.; Bresci, E.; Ouessar, M. Effect of Traditional Check Dams (Jessour) on Soil and Olive Trees Water Status in Tunisia. *Sci. Total Environ.* **2019**, *690*, 226–236. [[CrossRef](#)]

23. Rockström, J.; Barron, J.; Fox, P. Rainwater Management for Increased Productivity among Small-Holder Farmers in Drought Prone Environments. *Phys. Chem. Earth Parts A/B/C* **2002**, *27*, 949–959. [[CrossRef](#)]
24. Dile, Y.T.; Karlberg, L.; Daggupati, P.; Srinivasan, R.; Wiberg, D.; Rockstroem, J. Assessing the Implications of Water Harvesting Intensification on Upstream-Downstream Ecosystem Services: A Case Study in the Lake Tana Basin. *Sci. Total Environ.* **2016**, *542*, 22–35. [[CrossRef](#)]
25. Castelli, G.; Minelli, A.; Meron, T.; Bresci, E.; Yazew, E.; Gebreegziabher, T.; Sebhateab, M. Impacts of Rainwater Harvesting and Rainwater Management on Upstream Downstream Agricultural Ecosystem Services in Two Catchments of Southern Tigray, Ethiopia. *Chem. Eng. Trans.* **2017**, *58*, 685–690. [[CrossRef](#)]
26. Regaya, K. Etude Géologique de La Formation Des Limons de Matmata (Sud Tunisien). In *Revue des Sciences de la Terre*; INRST: Tunis, Tunisia, 1985; Volume 1.
27. Coudé-Gaussen, G. Les Poussières Sahariennes et Leur Contribution Aux Sédimentations Désertiques et Péri-désertiques. Ph.D. Thesis, Université Pierre et Marie Curie Paris 6, Paris, France, 1989.
28. Ben Fraj, T. La Jeffara Septentrionale: Étude de l'Évolution Géomorphologique Au Cours Du Quaternaire. Ph.D. Thesis, Faculté des Sciences Humaines et Sociales de Tunis, Tunis, Tunisia, 2012.
29. Ben Fraj, T. Proposition d'un Schéma Chronostratigraphique Des Héritages Quaternaires Continentaux de La Jeffara Septentrionale et de La Partie Nord-Orientale Du Plateau de Dahar-Matmata (Sud-Est Tunisien). *Quaternaire* **2012**, *23*, 187–204. [[CrossRef](#)]
30. Bonvallot, J. Tabias et Jessour Du Sud Tunisien: Agriculture Dans Les Zones Marginales et Parade à l'érosion. *Cah. ORSTOM Ser. Pedol.* **1986**, *22*, 163–171.
31. Floret, C.; Pontanier, R. *L'aridité En Tunisie Présaharienne: Climat, Sol, Végétation et Aménagement*; ORSTOM: Paris, France, 1982.
32. Henia, L. *Climat et Bilans de l'eau En Tunisie, Essai de Régionalisation Climatique Par Les Bilans Hydriques*; Publication de l'Université de Tunis: Tunis, Tunisia, 1993.
33. Institut National de la Météorologie. *Fiche Climatique de La Station de Beni Khedache 1990–2004*; Institut National de la Météorologie: Tunis, Tunisia, 2005.
34. Ben Ouedzou, H. Les Aménagements de Petite Hydraulique Dans Le Sud Tunisien, Un Savoir-Faire Traditionnel Au Service Du Développement Durable. In *Actes du Séminaire International «Patrimoine et Développement Durable en Méditerranée Occidentale»*; Institut National du Patrimoine: Tunis, Tunisia, 2002; pp. 45–54.
35. Bonvallot, J. Plaidoyer Pour Les Jessour. In *L'aridité: Une Contrainte au Développement. Caractérisation, Réponses Biologiques, Stratégies des Sociétés*; Le Floch, E., Grouzis, M., Cornet, A., Bille, J.-C., Eds.; Didactiques: Paris, France, 1992; pp. 507–517.
36. Ben Ouedzou, H.; Troussset, P. Aménagements Hydrauliques Dans Le Sud-Est Tunisien. In *Contrôle et Distribution de L'eau dans le Maghreb Antique et Médiéval*; Ecole Française de Rome: Rome, Italy, 2009; pp. 1–18.
37. Ouassar, M. Hydrological Impacts of Rainwater Harvesting in Wadi Oum Zessar Watershed (Southern Tunisia). Ph.D. Thesis, Ghent University, Ghent, Belgium, 2007.
38. FAO. *FAO World Reference Base for Soil Resources 2014: International Soil Classification System for Naming Soils and Creating Legends for Soil Maps*; World Soil Resources Reports; FAO: Rome, Italy, 2014.
39. Dean, T.J.; Bell, J.P.; Baty, A.J.B. Soil Moisture Measurement by an Improved Capacitance Technique, Part I. Sensor Design and Performance. *J. Hydrol.* **1987**, *93*, 67–78. [[CrossRef](#)]
40. Espitalie, J.; Deroo, G.; Marquis, F. Rock-Eval Pyrolysis and Its Applications (Part 2). *Rev. De L'institut Français Du Pétrole* **1985**, *40*, 755–784. [[CrossRef](#)]
41. Rawls, W.J.; Brakensiek, D.L.; Saxton, K.E. Estimating Soil Water Retention from Soil Properties. *J. Irrig. Drain. Eng.* **1982**, *108*, 166–171. [[CrossRef](#)]
42. Richards, L.A.; Weaver, L.R. Moisture Retention by Some Irrigated Soils as Related to Soil Moisture Tension. *J. Agric. Res.* **1944**, *69*, 215–235.
43. Gupta, S.C.; Larson, W.E. Estimating Soil Water Retention Characteristics from Particle Size Distribution, Organic Matter Percent, and Bulk Density. *Water Resour. Res.* **1979**, *15*, 1633–1635. [[CrossRef](#)]
44. Turc, L. Estimation of Irrigation Water Requirements, Potential Evapotranspiration: A Simple Climatic Formula Evolved up to Date. *Ann. Agron.* **1961**, *12*, 13–49.
45. Damagnez, J.; Riou, C.; De Villele, O.; El Amami, S. Estimation et Mesure de l'évapotranspiration Potentielle En Tunisie. *A.I.H.S.* **1963**, *62*, 98–119.
46. Clapp, R.B.; Hornberger, G.M. Empirical Equations for Some Soil Hydraulic Properties. *Water Resour. Res.* **1978**, *14*, 601–604. [[CrossRef](#)]
47. Šimanský, V.; Juriga, M.; Jonczak, J.; Uzarowicz, Ł.; Stepień, W. How Relationships between Soil Organic Matter Parameters and Soil Structure Characteristics Are Affected by the Long-Term Fertilization of a Sandy Soil. *Geoderma* **2019**, *342*, 75–84. [[CrossRef](#)]
48. Gruhier, C.; de Rosnay, P.; Hasenauer, S.; Holmes, T.; de Jeu, R.; Kerr, Y.; Mougou, E.; Njoku, E.; Timouk, F.; Wagner, W.; et al. Soil Moisture Active and Passive Microwave Products: Intercomparison and Evaluation over a Sahelian Site. *Hydrol. Earth Syst. Sci.* **2010**, *14*, 141–156. [[CrossRef](#)]
49. Milly, P.C.D. Potential Evaporation and Soil Moisture in General Circulation Models. *J. Clim.* **1992**, *5*, 209–226. [[CrossRef](#)]
50. Lü, H.; Zhu, Y.; Skaggs, T.H.; Yu, Z. Comparison of Measured and Simulated Water Storage in Dryland Terraces of the Loess Plateau, China. *Agric. Water Manag.* **2009**, *96*, 299–306. [[CrossRef](#)]

51. Xu, Y.; Zhu, G.; Wan, Q.; Yong, L.; Ma, H.; Sun, Z.; Zhang, Z.; Qiu, D. Effect of Terrace Construction on Soil Moisture in Rain-Fed Farming Area of Loess Plateau. *J. Hydrol. Reg. Stud.* **2021**, *37*, 100889. [[CrossRef](#)]
52. Yang, L.; Wei, W.; Chen, L.; Chen, W.; Wang, J. Response of Temporal Variation of Soil Moisture to Vegetation Restoration in Semi-Arid Loess Plateau, China. *CATENA* **2014**, *115*, 123–133. [[CrossRef](#)]
53. Gómez, J.A.; Llewellyn, C.; Basch, G.; Sutton, P.B.; Dyson, J.S.; Jones, C.A. The Effects of Cover Crops and Conventional Tillage on Soil and Runoff Loss in Vineyards and Olive Groves in Several Mediterranean Countries. *Soil Use Manag.* **2011**, *27*, 502–514. [[CrossRef](#)]
54. Coppola, A.; Abdallah, M.; Dragonetti, G.; Zdruli, P.; Lamaddalena, N. Monitoring and Modelling the Hydrological Behaviour of a Reclaimed Wadi Basin in Egypt. *Ecohydrology* **2019**, *12*, e2084. [[CrossRef](#)]
55. Sanz-Cortés, F.; Martínez-Calvo, J.; Badenes, M.L.; Bleiholder, H.; Hack, H.; Llacer, G.; Meier, U. Phenological Growth Stages of Olive Trees (*Olea Europaea*). *Ann. Appl. Biol.* **2002**, *140*, 151–157. [[CrossRef](#)]

Disclaimer/Publisher's Note: The statements, opinions and data contained in all publications are solely those of the individual author(s) and contributor(s) and not of MDPI and/or the editor(s). MDPI and/or the editor(s) disclaim responsibility for any injury to people or property resulting from any ideas, methods, instructions or products referred to in the content.